**République Algérienne Démocratique et Populaire**

**Ministère de l'Enseignement Superieure et de la Recherche Scientifique**

---

**Université Echahid Hamma Lakhdar d'El-Oued**

**FACULTE DE TECHNOLOGIE**

**DEPARTEMENT DE GENIE MECANIQUE**

## Mémoire de fin d'étude

Présenté pour l'obtention du diplôme de

# MASTER ACADEMIQUE

Domaine : Sciences et Technologies

Filière : Electromécanique

Spécialité : Electromécanique

## Thème

# Etude des techniques d'estimation de l'état de charge de la batterie d'un système embarqué

Devant le jury composé de :

| | |
|---|---|
| ……..…… | Président |
| ……..…….. | Examinateur |
| …….... | Examinateur |
| Mr. ZINE Bachir | Encadreur |

Présenté par :

- BIA Haithem
- KHADEM Bachir
- BELLILI Sifeddine

**2019-2020**

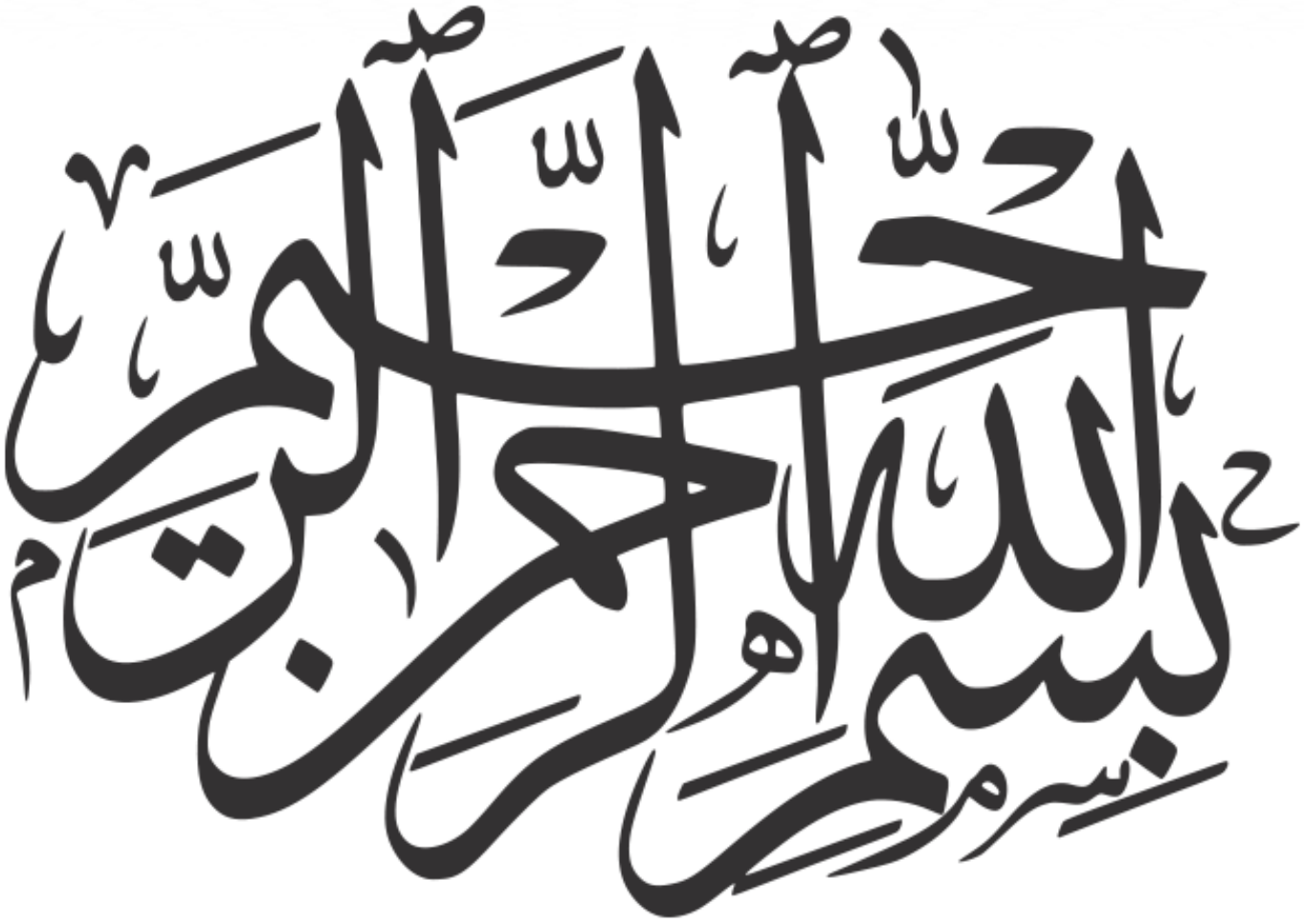


*BISMILLAHIR-RAHMANIR-RAHIM*

IN THE NAME OF ALLAH, THE COMPASSIONATE, THE MERCIFUL

# Acknowledgements

First of all, we hold our thanks to Allah for giving us strength and courage.

Following We would like to warmly thank

Sir. ZINE Bachir our supervisor who has made enormous efforts, through his information, advice and encouragement.

And all the professors of the Department of Mechanical Engineering
To all those who were at one time or at any time involved in this work.

We sincerely thank Dr. ZELOUMA Laid for helping us to carry out this work.

We thank all the farmers who helped us

Our warmest thanks to all those who from near and far have contributed to the realization of this thesis.

# Dedication

*We dedicate this modest thesis to our parents who were able to support us throughout our studies, sometimes comfort us in difficult times, and who without them we could not have done this work.*

*We dedicate this modest work:*

*To our brothers and sisters.*

*To all our family's.*

*To all our loyal friends.*

*To All our teachers since childhood.*

*To the entire 2020 promotion.*

*Our dedication also goes to those who have participated directly or indirectly in the culmination of our efforts.*

# Contents

## *Table of Contents*


| No. | Contents | Page |
|---|---|---|
| | List of Abbreviations | i |
| | List of Symbols | iii |
| | List of Figures | vii |
| | List of Tables | viii |
| | General Introduction | 1 |
| | **Chapter I: State-of-the-Art of Battery State-of-Charge** | |
| I.1 | Introduction | 2 |
| I.2 | A General State-of-Charge System | 2 |
| I.3 | Definition of General Battery Parameters | 3 |
| I.4 | State-of-the-Art of Battery State-of-Charge | 5 |
| I.4.1 | Direct Measurement | 5 |
| I.4.2 | Book-Keeping Systems | 9 |
| I.4.3 | Adaptive Systems | 12 |
| I.5 | Conclusion | 16 |
| | **Chapter II: Battery Modeling** | |
| II.1 | Introduction | 17 |
| II.2 | Electric Vehicle Battery Technologies | 17 |
| II.2.1 | Overview | 17 |
| II.2.2 | Basics of Lead Acid Battery | 17 |
| II.2.3 | Basics of Lithium-ion Battery | 18 |
| II.3 | Methods of Charging Electric Vehicle Battery | 20 |
| II.3.1 | Methods of Charging Lead-Acid Batteries | 20 |
| II.3.2 | Methods of Charging Lithium Batteries | 21 |
| II.3.3 | Common Methods to Charge Batteries | 24 |
| II.4 | Types of Battery Models | 26 |
| II.4.1 | Lead Acid Battery Models | 26 |
| II.4.2 | Lithium Battery Models | 29 |
| II.5 | Comparing Lithium-ion and Lead Acid Batteries | 35 |
| II.6 | Conclusion | 39 |
| | **Chapter III: Coulomb Counting Method Estimation** | |
| III.1 | Introduction | 40 |
| III.2 | Coulomb Counting Method | 40 |
| III.3 | Generic Battery Model | 41 |
| III.3.1 | State of the Art | 41 |
| III.3.2 | Charge/Discharge of this Model in MATLAB Simulink | 42 |
| III.4 | Application | 44 |
| III.5 | Simulation Results and Discussions | 45 |
| III.6 | Conclusion | 51 |

| | **Chapter IV: Results and Discussions** | |
|---|---|---|
| IV.1 | Introduction | 52 |
| IV.2 | Experimentation and Validation of Results | 52 |
| IV.2.1 | Description of the Test Bench | 52 |
| IV.2.2 | Test Procedure | 53 |
| IV.3 | Results and Discussions | 54 |
| IV.4 | Conclusion | 61 |
| | General Conclusion | 62 |
| | Appendices | 64 |
| | References | 67 |

# List of Abbreviations and Symbols

# List of Abbreviations

| Abbreviation | Definition |
|---|---|
| $ANN$ | Artificial Neural Networks |
| $AR_d$ | Actual Rate discharge current |
| $BMS$ | Battery Management System |
| $cc$ | Coulomb Counting |
| $CC$ | Constant-Current |
| $CV$ | Constant-Voltage |
| $Ch$ | Charge |
| $EMF$ | Electro-Motive Force |
| $EMF_F$ | EMF fitting method |
| $EKF$ | Extended Kalman Filters |
| $EMF_m$ | Measured EMF data points |
| $ISP$ | In-System Programming |
| $IF$ | In-Functional |
| $IC$ | Integrated Circuit |
| $Li-ion$ | Lithium-ion |
| $LA$ | Lead Acid |
| $Li-ion\ POL$ | Lithium-ion Polymer |
| $Li$ | Lithium |
| $NiCd$ | Nickel-Cadmium |
| $NiMH$ | Nickel-Metal Hybride |

| | |
|---|---|
| $NI$ | National Instruments |
| $SOH$ | State-of-Health |
| $n_m$ | Overpotential model |
| $SOC$ | State-of-Charge |
| $EMS$ | Energy Management System |
| $OCV$ | Open Circuit Voltage |
| $HEV$ | Hybrid Electric Vehicle |
| $HEV_s$ | Hybrid Electric Vehicles |
| $EV$ | Electric Vehicle |
| $EV_s$ | Electric Vehicles |
| $DC$ | Direct Current |
| $Ah$ | Ampere hour |
| $PV$ | Photovoltaic |
| $AGM$ | Absorbed Glass Matrix |
| $CC-CV$ | Constant-Current-Constant-Voltage |
| $PSO$ | Particle Swarm Optimization |
| $h$ | hours |
| $AC$ | Alternative Current |
| $R$ | Resistance |
| $C$ | Capacitance |
| $BATT$ | Battery |
| $E_{OC}$ | Charge of Open Circuit Voltage |

| | |
|---|---|
| $DOD$ | Depth of discharge |
| $SOC_s$ | State-of-Charge-Systems |
| $COV$ | Cut-of-Voltage |
| $SOC_{est}$ | State-of-Charge Estimed |
| $SOC_{bat}$ | State-of-Charge battery |
| $SOC_0$ | Initial State-of-Charge |

# List of Symbols

| Symbol | Definition | Unite |
|---|---|---|
| $DOD$ | Depth-of-Discharge | [%] |
| $DOC$ | Depth-of-Charge | [%] |
| $EMF$ | Electro-Motive Force | [V] |
| $E_q^0$ | Amount of the energy | [J] |
| $E_q^I$ | Non-linear part of the amount of the energy | [J] |
| $E_{eq}^+$ | Equilibrium potential of the positive electrode | [V] |
| $E_{eq}^-$ | Equilibrium potential of the negative electrode | [V] |
| $E_0^+$ | Standard redox potential of the positive electrode | [V] |
| $E_0^-$ | Standard redox potential of the negative electrode | [V] |
| $E_0$ | Parameter for the SOC-EMF | [V] |
| $EMF_P$ | Predicted EMF voltage | [V] |
| $EMF_F$ | Flited EMF | [V] |
| $F$ | Faraday Constant | [C/mol] |
| $f$ | Frequency | [Hz] |

| | | |
|---|---|---|
| $I_s^{max}$ | Constant maximum current | [A] |
| $I_s^{min}$ | Predefined minimum current | [A] |
| $I_M$ | Uncertainties from Maccor current measurement | [A] |
| $I_S$ | Standby current | [A] |
| $I_d$ | Measured discharge current | [A] |
| $n_0$ | Parameter related to the magnitude of the diffusion overpotential | - |
| $n_1$ | Parameter related to the magnitude of the diffusion overpotential | [1/T] |
| $OCV$ | Open-Circuit-Voltage | [V] |
| $OCV_f$ | Battery OCV for a fresh battery | [V] |
| $OCV_a$ | Battery OCV for an aged battery | [V] |
| $Q_{in}$ | Charge present in the battery at the time t | [Ah] |
| $Q_{max}$ | Battery maximum capacity | [Ah] |
| $Q_d$ | Discharge battery capacity | [Ah] |
| $Q_{max}^+$ | Maximum capacity of the positive electrode | [1] |
| $Q_{max}^-$ | Maximum capacity of the negative electrode | [1] |
| $Q_{ch}$ | Amount of charge flowing into the battery during the charge state | [Ah] |
| $Q_d$ | Discharge capacity | [A] |
| $R_S$ | Sens resistor | [$\Omega$] |
| $SOC$ | State-of-Charge | [%] |
| $SOC_{(EMF)}$ | SOC calculated based on the EMF voltage | [%] |
| $SOC_{(vp)}$ | SOC Calculated based on the predicted voltage | [%] |
| $SOC_e$ | SOC error | [%] |

| | | |
|---|---|---|
| $SOC_{end}$ | SOC indicated at the end | [%] |
| $SOC_{in}$ | SOC in the initial state | [%] |
| $SOC_{ch}$ | SOC in the charge state | [%] |
| $t$ | Time | [s] |
| $T$ | Temperature | [°C] |
| $T_{ref}$ | Reference temperature | [°C] |
| $V_{bat}$ | Battery terminal voltage | [V] |
| $V$ | Battery voltage | [V] |
| $V_d$ | Battery voltage after discharging | [V] |
| $V_{ch}$ | Battery voltage after charging | [V] |
| $V_M$ | Uncertainties from Maccor voltage measurement | [V] |
| $V_0$ | Battery voltage at t=1min | [V] |
| $V_{ocf}$ | Fully stabilized Open-Circuit-Voltage | [V] |
| $V_s^{max}$ | Maximum charge voltage in CV | [V] |
| $V_{off}$ | Voltage offset | [V] |
| $\gamma$ | Rate-determing variable | - |
| $\delta$ | Parameter in the voltage prediction model | - |
| $\Gamma$ | Constant for voltage prediction | - |
| $\eta_{ch}$ | Charge overpotential | [V] |
| $\eta_d$ | Discharge overpotential | [V] |
| $\eta_f$ | Overpotential model parameters for a fresh battery | [V] |
| $\eta_{ch}^a$ | Measured charge overpotential for an aged battery | [V] |

| | | |
|---|---|---|
| $\eta_{ch}^{f}$ | Measured charge overpotential for a fresh battery | [V] |
| $\phi$ | Phase angle | [rad] |
| $\tau$ | Voltage relaxation time | [s] |
| $\tau_q$ | Time constant associated with the increase in overpotential in almost empty battery | [s] |
| $\tau_d$ | "Diffusion" time constant | [s] |
| $k_0$ | Standard rate constant for heterogeneous reaction | - |
| $\alpha$ | Transfer coefficient | - |
| $c$ | Concentration at the surface of the electrode | - |

# List of Figures and Tables

# List of Figures


| No. | Figure | Page |
|---|---|---|
| Fig.I.1 | General Pratical Architecture of State-of-Charge System [6] | 3 |
| Fig.I.2 | Basic Precept of a SOC Indication System Based Totally on Direct Measurement [4] | 6 |
| Fig.I.3 | Li-ion Battery Voltage Curves at Different Discharge Rates[9] | 6 |
| Fig.I.4 | Bookkeeping Support Module (BKM) Block Diagram [4] | 11 |
| Fig.I.5 | Battery Voltage Estimated Compared With The Measured Battery Voltage [12] | 12 |
| Fig.I.6 | Schematic Representation of Smart Battery Management using ANN [15] | 13 |
| Fig.II.1 | Lithium-ion Reaction [24] | 19 |
| Fig.II.2 | Five-step Charging Pattern [32] | 22 |
| Fig.II.3 | PSO Updating Concept [32] | 23 |
| Fig.II.4 | AC Impedance Model [7] | 26 |
| Fig.II.5 | Equivalent Circuit Model of Simple Model [41] | 27 |
| Fig.II.6 | Equivalent Circuit Model of Thevenin Model [42] | 27 |
| Fig.II.7 | Equivalent Circuit of Copetti Model [43] | 28 |
| Fig.II.8 | Circuit Structure of Rint Model [44] | 29 |
| Fig.II.9 | Circuit Structure of Thevenin Model [45] | 29 |
| Fig.II.10 | Circuit Structure of RC Model [46] | 30 |
| Fig.II.11 | Circuit Structure of PNGV Model [46] | 30 |
| Fig.II.12 | The Dispersion Effect in Electrochemical Impedance Spectroscopy [47] | 32 |
| Fig.II.13 | Lithium-ion Safety Mechanisms [57] | 37 |
| Fig.III.1 | Battery Charged Discharge Pattern | 43 |
| Fig.III.2 | Discharging Voltage as a Function of Time at '0.25C' | 45 |
| Fig.III.3 | State of Charge as a Function of Time at '0.25C' | 46 |
| Fig.III.4 | Discharging Voltage as a Function of Time at '0.17C' | 46 |
| Fig.III.5 | State of Charge as a Function of Time at '0.17C' | 47 |
| Fig.III.6 | Discharging Voltage as a Function of Time at '0.09C' | 48 |
| Fig.III.7 | State of Charge as a Function of Time at '0.09C' | 48 |
| Fig.III.8 | Charging Current as a Function of Time | 49 |
| Fig.III.9 | Charging Voltage as a Function of Time | 50 |
| Fig.III.10 | The State of Charge as a Function of Time 'Charge Test ' | 50 |
| Fig.IV.1 | Test Bench | 52 |
| Fig.IV.2 | The Discharge Voltage as a Function of Time at 0.25C | 54 |
| Fig.IV.3 | The State of Charge of the Battery (SOC) as a Function of Time at 0.25C | 55 |
| Fig.IV.4 | The Discharge Voltage as a Function of Time at 0.17C | 55 |

| | | |
|---|---|---|
| Fig.IV.5 | The State of Charge of the Battery (SOC) as a Function of Time at 0.17C | 56 |
| Fig.IV.6 | The Discharge Voltage as a Function of Time at 0.09C | 57 |
| Fig.IV.7 | The State of Charge of the Battery (SOC) as a Function of Time at 0.09C | 58 |
| Fig.IV.8 | The Charge Current as a Function of Time | 58 |
| Fig.IV.9 | The Charge Voltage as a Function of Time | 59 |
| Fig.IV.10 | The State of Charge of the Battery (SOC) as a Function of Time | 60 |
| Fig.A.1 | GPL 12520 12V 52Ah Battery Picture | 64 |
| Fig.A.2 | Specifications in Our Battery Model | 65 |
| Fig.A.3 | Float Service Life | 66 |
| Fig.A.4 | Capacity Retention | 66 |
| Fig.A.5 | Battery Voltage and Charge Time for Standby Use | 66 |
| Fig.A.6 | Cycle Service Life | 66 |
| Fig.A.7 | Battery Voltage and Charge Time for Cycle Use | 66 |
| Fig.A.8 | Terminal Voltage (V) and Discharge Time | 66 |


# List of Tables


| No. | Table | Page |
|---|---|---|
| Table I.1 | Overview of Methods for SOC Determination [18] | 15 |
| Table II.1 | Lead Acid Charge States [22] | 18 |
| Table II.2 | Lithium-ion Subcategory Comparison [27,28] | 20 |
| Table II.3 | Battery Technology Comparison [29,52,53] | 35 |
| Table II.4 | Advantages and Limitations of Lead Acid Batteries [59,60] | 38 |
| Table II.5 | Advantages and Limitations of Li-ion Batteries [59,60] | 39 |
| Table III.1 | Parameters of Our Battery at 0.25C | 44 |
| Table III.2 | Parameters of Our Battery at 0.17C | 44 |
| Table III.3 | Parameters of Our Battery at 0.09C | 45 |
| Table A.1 | Charging Procedure | 65 |
| Table A.2 | Discharge Current VS Discharge Voltage | 65 |

# General Introduction

# General Introduction

In today's society, high importance is being placed on the stress levels that technology puts on the environment. This factor has pushed automobile technology to an eco-friendlier solution which is electric vehicles (EV) [1]. When compared to petroleum-based vehicles using the internal combustion engine (ICE), EVs have a significantly less footprint depending on their fuel source [2].

In an EV, batteries store the electrical energy in an electrochemical reaction for later use. There are several types of batteries in the industry. The most popular are lead-acid, nickel, alkaline and lithium-ion [1]. Lithium has become very popular because it is light metal, has the greatest electrochemical potential and provides the largest specific energy per weight [1].

In addition, the SOC and voltage measurement from the cell's terminal is crucial information to determine the available energy in the battery, which can be used to determine the available driving range of the EV. Unfortunately, it is not possible to have direct measurements of the SOC [2]. The main difficulties are listed below:

- The battery pack of EVs has hundreds of cells connected in series, the different accumulated potential of each cell is different to each other making it hard to have unified compensation or elimination methods.
- Voltage measurement requires high precision as other parameters are estimated based on the voltage measurement. Required voltage precision is around 1 mV to have low carried % errors [3].

The aim of this work is to develop a battery charge estimator based on a charge / discharge test campaign in order to develop an accurate estimator. This estimate will depend on the battery technology, its electrical characteristics but also the ambient temperature.

This thesis is divided into four chapters, in the first chapter, gives a state of the art on the state-of-charge indicator, some definitions of SOC and principles of some SOC estimation techniques. The second chapter presents the battery modeling . The third chapter is devoted to the theoretical study of the coulomb counting and its application to estimate SOC from experimental measurements of voltage, current and of the temperature. The fourth chapter concerns all results and discussions based on our theoretical and practical experiences.

# Chapter I:

# State-of-the-Art of Battery State-of-Charge

## I.1. Introduction

The state of charge (SOC) is one of the essential factors to characterize the state of storage elements. Its knowledge is all the more critical for the Liion battery, as a poorly controlled charge for this technology can lead to the destruction of the accumulator [4].

In this chapter we will give the history of the SOC indicator, some definitions of SOC, battery management system, the principle of the different SOC techniques including direct methods; adaptive methods and finally methods hybrids.

## I.2. A General State-of-Charge System

In science, the quality unit want to communicate battery limit is Coulomb (named when the French scientist C. A. Coulomb, 1736–1806), that portrays the time a battery will produce a given current. The Coulomb is that the unit of electrical charge like one quantity unit (As).

In observe, however, cell or battery capability is a lot of usually expressed in ampere-hours (Ah) or milliampere-hours (mAh). Of nice importance for users is to understand a battery's SOC. In [5] SOC is defined as the percentage of the full capacity of a battery that is still available for further discharge. In [6] it is the ratio of a cell's available capacity and its maximum attainable capacity. For a correct understanding of what the term 'SOC' extremely implies a transparent definition is needed; SOC is the percentage of maximum possible charge that is present inside a rechargeable battery. The SOC measuring methodology and also the machine model supported the right SOC definition should be straightforward, convenient, sensible and reliable.

Fig. I.1 suggests an instance of a sensible SOC system. The battery may also encompass a plurality of battery cells related in sequence and/or parallel, every of the battery cells having at least two terminals. The SOC device may additionally include an analogue-to-digital converter (ADC) for converting a voltage drop between at least two feel resistor connection pins as a measure of the modern-day (I) into a digital sign and also for changing the measured analogue values of the battery voltage (V) and temperature (T) into digital signals.

A microprocessor/microcontroller (in which the SOC algorithm is stored) determines a battery system's SOC on the groundwork of the measured signals. Two sorts of reminiscence are needed. Basic battery data, such as the amount of self-discharge as a function of T and the discharging efficiency as a feature of I and T, are read from the read-only reminiscence (ROM).

When the SOC algorithm is primarily based on EMF measurements, the EMF–SOC relationship can be saved in ROM collectively with different battery-specific data. The random

get right of entry to reminiscence (RAM) is used to save the history of use, such as the quantity of charge/discharge cycles, which can be used to replace the most battery capacity. Each part of this system (software algorithm or hardware device) will have an effect on the last accuracy of the SOC indication (e.g. inaccuracy in the V, T and I measurements will result in inaccuracy in the closing SOC). Also essential is the calibration of the SOC, because if the SOC algorithm is based on, say, present day size and integration, the error triggered via the cutting-edge measurement inaccuracy will accumulate over time.

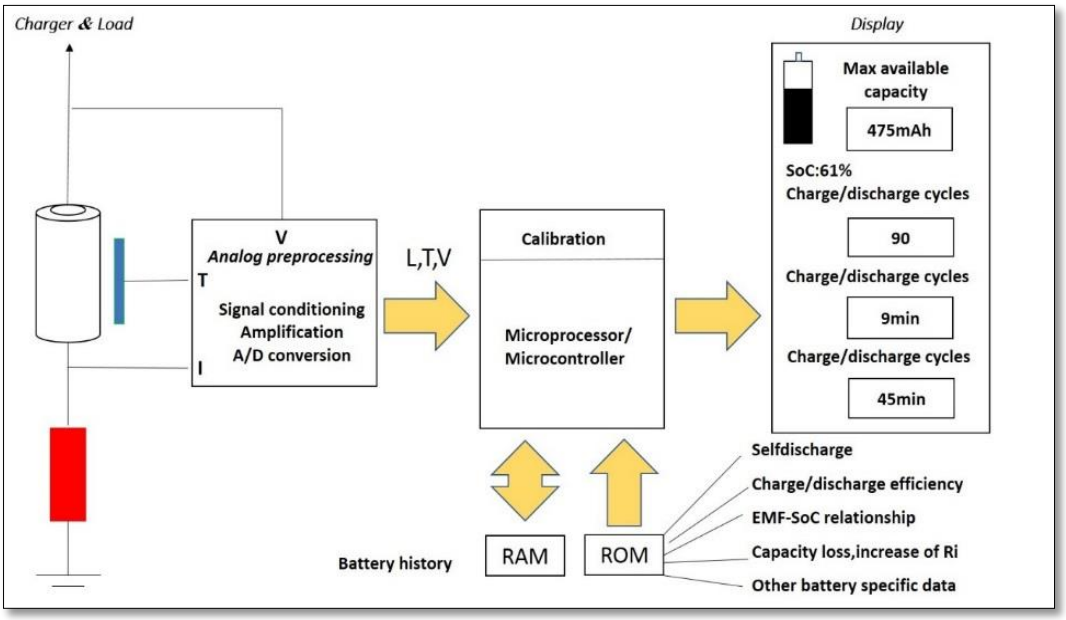


**Figure I.1:** *General Practical Architecture of a State-of-Charge System [6].*

## I.3. Definition of General Battery Parameters

For an environment friendly dialogue of SOC indication methods, some of the phrases frequently used in the battery SOC should be defined.

- **Ampere-hour.** A measure of electric powered charge described as the imperative product of present day (in Amperes) and time (in hours).
- **Cell.** The fundamental electrochemical unit used to generate electrical strength from saved chemical electricity or to save electrical electricity in the form of chemical energy. A cell consists of two electrodes in a container stuffed with an electrolyte.
- **Battery.** Two or extra cells related in a fantastic series/parallel arrangement to acquire the working voltage and capacity required for a certain load. The term is additionally often used for single cells.

- **Li-ion cells.** Cells containing a liquid organic or polymer electrolyte in which the anode and cathode are both made of intercalation compounds [7].
- **C-rate.** A charge or discharge contemporary = in Amperes to the rated potential in Ah. Multiples larger or smaller than the C-rate are used to categorical larger or smaller currents. For example, the C-rate is 1100 mA in the case of an 1100 mAh battery, while the C/2 and 2C-rates are 550 mA and 2.2 A, respectively.
- **Capacity.** A battery's electrical power content material expressed in ampere-hours.
- **Maximum capacity.** Maximum amount of ability that can be removed from a battery below defined discharge conditions.
- **Cycle life.** The number of cycles that a cell or battery can be charged and discharged under specific conditions before the available ability in Ah fails to meet particular performance criteria. This will normally be 80% of the rated capacity.
- **Cut-off voltage.** The lowest operating voltage at which a cell is considered depleted. Also often referred to as end-of-discharge voltage or final voltage [8].
- **Self-discharge.** The recoverable loss of a cell's beneficial ability on storage due to interior chemical action. This is normally expressed in a share of the rated capacity lost per month at a sure temperature because batteries' self-discharge prices are strongly temperature-dependent. The self-discharge mechanism is a local redox process caused by decomposition of the electrolyte [7]. Other vital sources for the self-discharge are micro-shorts and shuttle-molecules.
- **Spread.** Difference between characteristics of batteries of the same type.
- **State-of-Health (SOH).** A 'measurement' that reflects a battery's regular situation and its capability to supply the detailed overall performance in contrast with a fresh battery.
- **State-of-Charge (SOC).** The percentage of the maximum viable cost that is current inside a rechargeable battery.
- **Depth-of-Discharge (DoD).** The amount of ability withdrawn from a battery expressed as a share of its most capacity.
- **Depth-of-Charge (DOC).** The quantity of potential put into a battery expressed as a proportion of its maximum capacity.
- **Remaining run-time.** The estimated time that a battery can grant modern to a transportable machine under legitimate discharge conditions before it will end functioning.

## I.4. State-of-the-Art of Battery State-of-Charge

As indicated, there are countless strategies for identifying the SOC of a battery. Some early, very inexpensive gasoline gauges simply measured voltage. Battery voltage is a relatively inaccurate indication of a battery's potential due to the fact it changes with temperature, discharge prices and aging. Another acknowledged technique for measuring SOC involves impedance measurements. The measurements received are in contrast with in the past generated fashionable reference curves. Yet every other prior-art technique used to determine battery SOCs involves estimating the SOC on the foundation of a battery's response to cutting-edge or voltage pulses. These pulse systems yield only a very accepted influence of a SOC and are used primarily to decide whether a battery is nevertheless useable. This first team of techniques will be called direct measurements below.

Another known method is to measure the current flowing into and out of a battery and to integrate this current over time in order to determine its capacity [4]. When the usage of these modern integrators one must correct the estimation of the SOC acquired because a number of battery-related elements have an effect on the accuracy of the estimation. These elements consist of temperature, history, cost and discharge efficiencies and cycle life. The integration of current is referred to in the literature as *Coulomb counting [4]*. When discharging 'efficiency', self-discharge and capacity loss are compensated for, this method can be regarded as a *book-keeping* system [4].

The foremost trouble in designing a correct SOC indication system is the unpredictability of the behavior of both batteries and users. For this reason use must be made of an adaptive system based on direct measurement, book-keeping or a combination of the two [4]. In order to clarify all aspects, these techniques will be discussed one after the other below.

### I.4.1. **Direct Measurement**

The direct dimension approach refers to the size of battery variables such as the battery voltage (V), battery impedance (Z) and voltage rest time (τ) after utility of a present-day step. Most relations between battery variables and the SOC rely on the temperature (T). This means that the battery temperature has to additionally be measured, except the voltage or impedance. The basic precept of a SOC indication system based on direct dimension is proven in Fig. I.4.

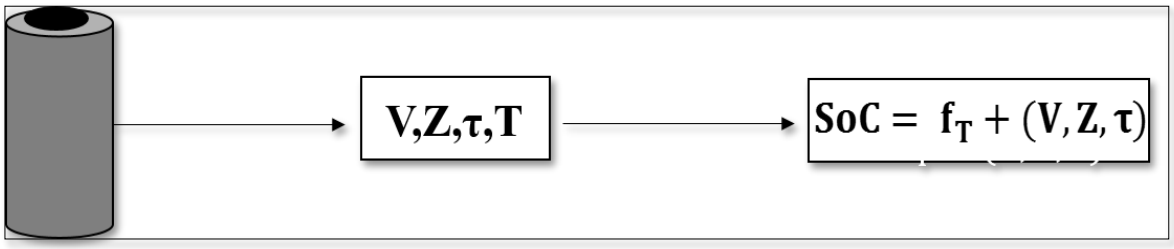


**Figure I.2:** *Basic Precept of a SOC Indication System Based Totally on Direct Measurement [4].*

The primary gain of a machine based on direct measurement is that it does not have to be constantly related to the battery. The measurements can be performed as soon as the battery has been connected [4].

Voltage measurements. Although voltage measurement has been a famous method, mainly for cell applications, it does no longer produce the most accurate results. Determining the remaining capacity of a cell simply by measuring its voltage level may be less expensive and may use less computing power of the host CPU than Coulomb counting, but under real-life conditions voltage measurements alone can be very misleading [9]. While it is authentic that a given cell voltage level will continually drop at some point of discharge, the voltage degree in relation to final charge varies radically with cell temperature and discharge rate. Fig. I.3 shows a Liion battery voltage curve during discharge at exceptional discharge rates.

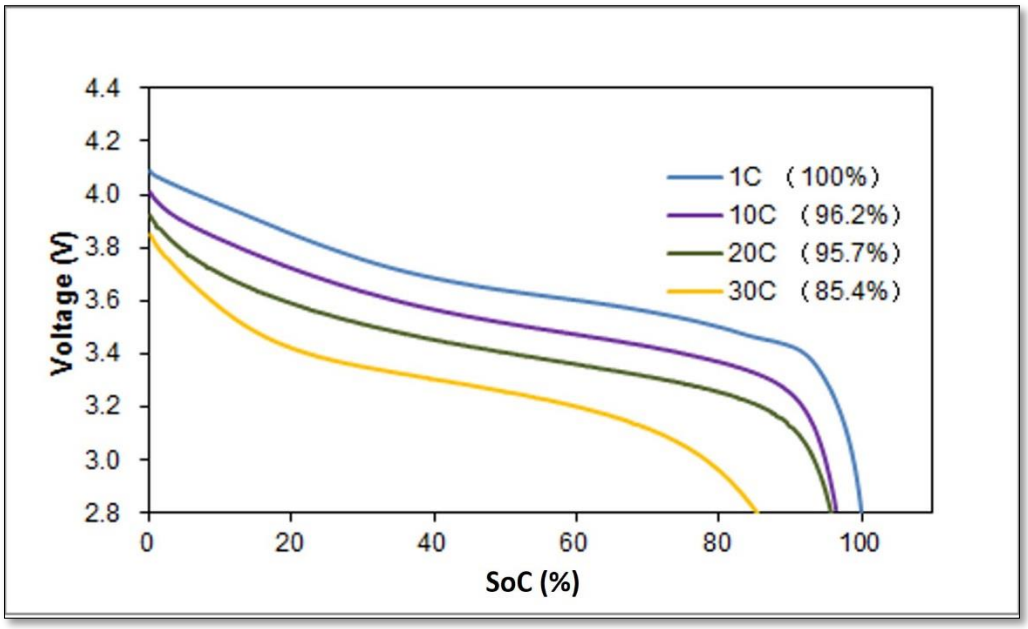


**Figure I.3:** *Li-ion Battery Voltage Curves at Different Discharge Rates [9].*

The significant point shown in Fig. I.3 This is the relation between the voltage of the cell and its discharged power. The voltage discharge curve can be seen to strongly depend on the rate of discharge. The device will correct the error in SOC calculation based on voltage measurement, if the battery voltage dependence on cell temperature and discharge rate is known. However, when those measured curves are included the process becomes more complicated and expensive than a Coulomb counting approach [9].

- *The EMF method.* The acronym EMF reflects electromotive force. It is the internal driving force of a battery for supplying energy to a charge. In principle, the EMF can be inferred from thermodynamic data and the Nernst equation (or equations derived from it) [4]. Another approach with which the EMF can be got is referred to as linear interpolation. With this method the common battery voltage, calculated at the identical SOC, is inferred from the battery voltages all through two consecutive discharge and charge cycles the usage of the equal currents and at the equal temperature.

In another known method the EMF is determined on the basis of *voltage relaxation*. The battery voltage will relax to the EMF value after current interruption. This may take a long time, especially when a battery is almost empty, at low temperatures and after a high discharge current rate [9]. In another EMF determination method – *linear extrapolation* – the battery voltages obtained with different currents with the same sign and at the same SOC value are linearly extrapolated to a current of value zero [4].

When the SOC algorithm is based on the EMF an accurate method for EMF implementation is required. Three of the EMF implementation methods used in exercise will be presented below.

- (a) *Look-up table.* A table in which fixed values of the measured parameters can be saved and used in order to point out SOC. The dimension and accuracy of the look-up tables in SOC indication systems depend on the quantity of saved values. One of the fundamental drawbacks of this method is that even in the case of a single type of battery it is tough to take into account each and every point of the EMF curve in order to furnish an accurate SOC indication system. When many dimension points are blanketed the technique turns into greater intricate and highly-priced than different approaches, and will likely now not supply any sizable advantages.
- (b) *Piecewise linear function.* In this technique the EMF curve is approximated with piecewise linear functions.

With the useful resource of Eq. (I.1), the SOC for any measured battery equilibrium voltage value, i.e. EMF, can be calculated:

$$\boldsymbol{SOC = SOC_1 + \frac{EMF - V_1}{V_h - V_1}(SOC_h - SOC_1)} \quad \textbf{(I.1)}$$

When adequate voltage and SOC intervals are chosen, this technique will allow more flexibility (possibility of implementation for different sorts of battery) and precision in SOC estimation based on the EMF curve in evaluation with a look-up table implementation. The troubles of spread, temperature and growing old remain to be solved.

- (c) *Mathematical function.* In this approach a mathematical equation is approximated to the EMF curve.

Using an adaptive approach to update the equation parameters, taking into account factors such as battery distribution, temperature and age, this method is likely to offer the best solution for a practical implementation of EMF.

- *Impedance measurements.* In general, the combination of a complex voltage and complex current is a complex quantity. The ratio *V/I* is generally denoted as the impedance *Z* [10]. This definition is not always correctly applied in the battery-related literature [11]. A useful way of researching processes in electrochemical systems like biological processes, batteries and capacitors is to make impedance measurements over a broad range of frequencies, usually referred to as Electrochemical Impedance Spectroscopy (EIS).

The electrochemical impedance (or ac impedance) of a battery characterizes its dynamic behavior, that is, its response to an excitation of small amplitude. In principle, any kind of excitation signal can also be used (sine wave, noise, step, . . .). In practice, sine waves are then again commonly used. In galvanostatic (constant current) mode, the dc modern I (polarization current) charging or discharging the battery is modified the use of a sinusoidal current:

$$\boldsymbol{\Delta I = I_{max}\sin(2\pi f t)} \quad \textbf{(I.2)}$$

at frequency *f*, which is superimposed to *I*, yielding a sinusoidal voltage response:

$$\boldsymbol{\Delta V = V_{max}\sin(2\pi f t + \phi)} \quad \textbf{(I.3)}$$

around the dc voltage *V* at the battery's terminals. The amplitude *V*max and the phase angle ∅ depend on the frequency *f* and *V*max also depends on the amplitude *I*max of the applied ac current. In contrast, in potentiation mode (constant voltage), the dc voltage *V* at the battery's terminals is modified using a sinusoidal voltage:

$$\Delta \boldsymbol{V} = \boldsymbol{V_{max}} \sin(2\pi \boldsymbol{f t}) \quad \textbf{(I.4)}$$

at frequency *f*, which is superimposed onto *V*, yielding a sinusoidal current response:

$$\Delta \boldsymbol{I} = \boldsymbol{I_{max}} \sin(2\pi \boldsymbol{f t} - \boldsymbol{\phi}) \quad \textbf{(I.5)}$$

around the dc current *I* flowing through the battery. In this case, the amplitude *Imax* and the phase angle ∅ depend on the frequency *f* and *Imax* also depends on the amplitude *Vmax* of the applied ac voltage. In both cases, the impedance is defined by

$$\boldsymbol{Z(f)} = \frac{\boldsymbol{V_{max}}}{\boldsymbol{I_{max}}} \boldsymbol{e^{j\varphi}} \quad \textbf{(I.6)}$$

Therefore, the electrochemical impedance of a battery is a frequency-dependent complex number characterized by either its real and imaginary parts or its modulus and phase angle ∅.

### I.4.2. **Book–keeping Systems**

Book-keeping is a method for SOC indication that is primarily based on both cutting-edge measurement and integration. This can be denoted as Coulomb counting, which actually means 'counting the charge flowing into or out of the battery'. These Coulomb counting facts and other applicable information of the battery such as self-discharge rate, temperature, charge/discharge efficiency, history (e.g. cycle life), etc. will be used as enter for the book-keeping system. The following Li-ion battery effects can be compensated for in a book-keeping system [4]:

- *Discharging 'efficiency'*. Depending generally on the SOC, T and I, solely part of the available cost interior a battery can be retrieved. The essential mechanisms in the back of this 'efficiency' are response kinetics and diffusion processes. These mechanisms contain reaction-rate and diffusion constants, which are temperature-dependent. Moreover, improved depletion of reacting species at the electrode surfaces occurs at larger currents and reaction-rate constants change over time as a battery age. Consequently, a battery that may appear empty after it has been discharged with a highly high contemporary can still be discharged in addition after a rest period and/or with a lower current. In general, much less charge can be obtained from a battery at low temperatures and/or large discharge currents. A battery's age also influences the discharging efficiency, for instance due to expanded inner resistance.

- *Self-discharge*. Any battery will gradually free charge, which will grow to be obvious when a battery is left unused for some time. A Coulomb counter cannot measure this volume of cost as no net current flows thru the battery terminals. A battery's self-discharge fee will depend strongly on temperature and on the SOC.
- *Capacity loss*. For Ah, the average battery capacity possible decreases when a battery age. The lack of ability depends on many factors. In general, the more the battery is misused, for example overcharged and over discharged on a regular basis, the larger the loss will be. In most commercial book-keeping systems voltage measurement is often used to update the maximum battery capacity so as to deal with capacity loss [4].

The general accuracy of 'Coulomb counting' depends on the accuracy of the modern measurement across the full operating range of the battery system, in both the charging and discharging modes. Typically, the present-day measuring machine measures the voltage throughout a shunt resistor related in collection to the battery machine and converts the measured voltage into a current. This cutting-edge is integrated and used to decide the SOC of the battery system. Higher cutting-edge stages require significantly decrease shunt resistor values and greater electricity dissipation ratings. The low resistance of such a shunt effects in a very small voltage drop throughout the shunt, which have to be measured in order to decide the smaller cost and discharge currents in the battery system. Since the characteristic of the battery monitoring system is to supply time integration of the battery modern in order to track the battery's SOC, even small errors in the size of the cutting-edge can motive large errors in the SOC measurement to accumulate over time. One of the frequent mistakes when the indicators to be measured are definitely small is the offset of the modern-day measurement device.

The book-keeping module (BKM) continuously monitors the battery and reports the obtained information (voltage, temperature, cutting-edge measurements and integration) to the processor. The processor makes use of this information and the battery identification facts to decide the SOC. The battery identification information consists of data allowing the dedication of the battery's capacity. That information is saved in the electrically erasable ROM (EEPROM) and are constantly up to date with the aid of the processor. The processor uses one-wire interface to speak with the battery. This means that the battery pack desires only three output connections: battery power, floor and one-wire interface.

The BKM can work in two different modes:

- ✓ *The sensitive mode*. When a cell is in idle mode, its output will be small so it will require greater accuracy to calculate the current. Sensitive mode requires a high sensitivity test.

- ✓ *The normal mode.* Compared to idle mode the consumption current is quite high during contact. For charge mode the standard mode is also used.

An excessive sensitivity, referred to as the lowest current value that wishes to be measured, is very important for making sure that all the cost flowing from and to a battery is monitored. The minor charge versions are not essential for users, but they are quintessential for the system's reliability. The gadget should have some inner registers (see Fig. I.4) that accumulate the minor variations. These registers are described below.

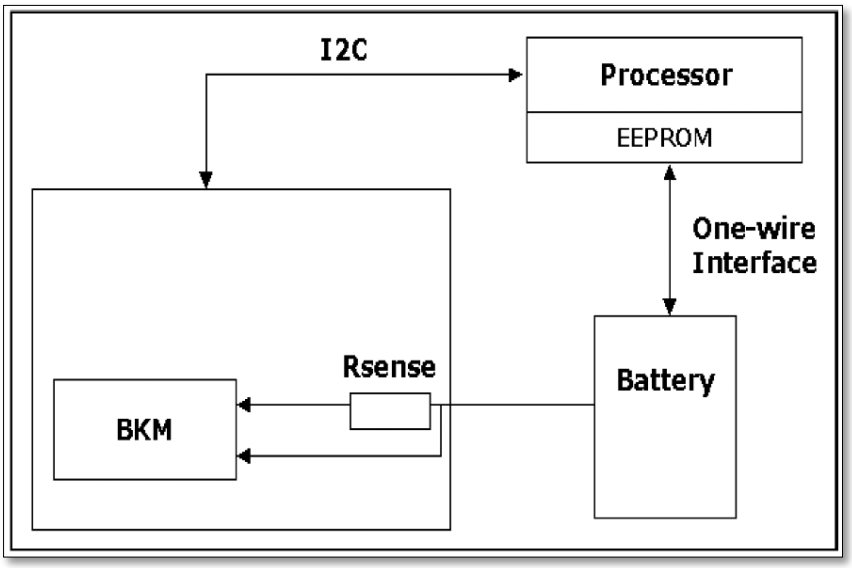


**Figure I.4:** *Bookkeeping Support Modul (BKM) Block Diagram [4].*

- ✓ *Current register*. Measurement at the moment of measurement of the current flowing into and out of a battery.
- ✓ *SOC (SOC counter)*. Maintains a net charge accumulated which flows into and out of a battery. Reading in this log is an example of the capacity left over. Every time a low indication is given this register is reset.
- ✓ *CCA (charging current accumulator)*. Accumulates the average charging current over the entire life of a battery. It is only enabled upon receiving current from the battery.
- ✓ *DCA (discharging current accumulator).* Accumulates the average discharging current over the life of a battery. It's only modified when current is given by the battery.

The DCA and CCA registers provide details on the battery system needed to determine the rechargeable battery's end-of-life, based on total charge / discharge current over its lifespan.

### I.4.3. **Adaptive Systems**

The main problem in developing a precise SOC signal device is the unpredictability of battery activity as well as user behavior. For this reason an adaptive system has to be used, which is based on direct measurement, book- keeping or a combination of the two [4]. This section will detail some examples of current adaptive SOC systems.

In [12], [13, 14] optimum Kalman filters are presented for implementing an adaptive method in connection with parameter estimation to determine SOC. The basis of the filter is a numeric battery model description. In [12] the battery voltage is estimated on the basis of current and temperature measurements and then the results are compared with the measured battery voltage value (see Fig. I.5).

The inner (internal) parameter contains at least the SOC, however could additionally include additional battery variables, such as an estimated value of the battery collection resistance (which will give data on the battery's SOH). The model may additionally incorporate the direct size feature or the book-keeping feature or an aggregate of the two. The system starts with a simple set of information describing well-known behavior of the kind of battery concerned.

Adaptivity of the model is based on a comparison of the estimated values with found battery behavior. This evaluation is made whenever possible. The cause of a Kalman filter is to estimate a system's kingdom on the groundwork of measurements, which include errors. The filter has the advantage of being sequential – it needs only the gadget variables of the previous pattern and the forcing terms and observations of the current sample.

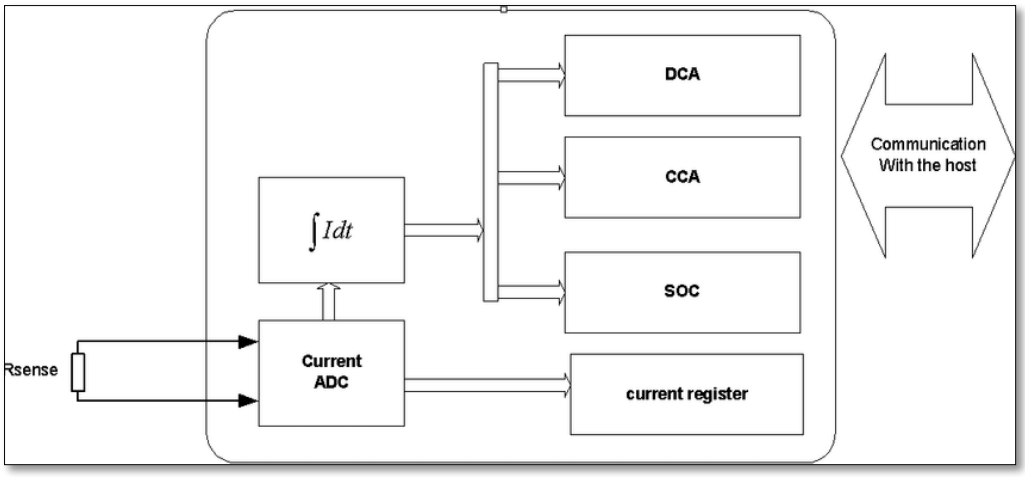


**Figure I.5:** *Battery Voltage Estimated Compared With the Measured Battery Voltage [12].*

In [13, 14] Plett shows how the EKF (extended KF) may be used to adaptively identify unknown parameters in a cell model, in real-time, given cell voltage, current and temperature measurements. Five mathematical state-space models for modelling LiPB hybrid electrical vehicle (HEV) cell dynamics are discussed. The fashions with a single kingdom are simple, but operate poorest. Adding hysteresis and filter states to the model improves performance, at some value in complexity. The last model includes phrases that describe the dynamic contributions due to open-circuit voltage, polarization time constants, electrochemical hysteresis, ohmic loss and the results of temperature. The results reveal that it is feasible to reap a root-mean-squared modelling error that is smaller than the level of quantization error anticipated in an implementation. It is concluded that EKF provides the best solution for long-term SOC estimation [13].

A battery's 'state variables' are replaced with neural weights with the aim of providing the portable equipment user with an accurate estimation of the remaining working time, *i.e.* how much time is left until the battery voltage reaches the cut-off value [15].

Two artificial neural networks (ANN), ANN_A and ANN_O, are used to model the system's implementation, more precisely to adapt the prediction of the present-day discharge curve to the everyday behavior of the employed battery pack (see Fig. I.6). An ANN requires at least two phases: a coaching segment to set the synaptic weights at these offering the 'best compromise' and a contrast segment to test the accuracy of the ANN the use of before unseen samples.

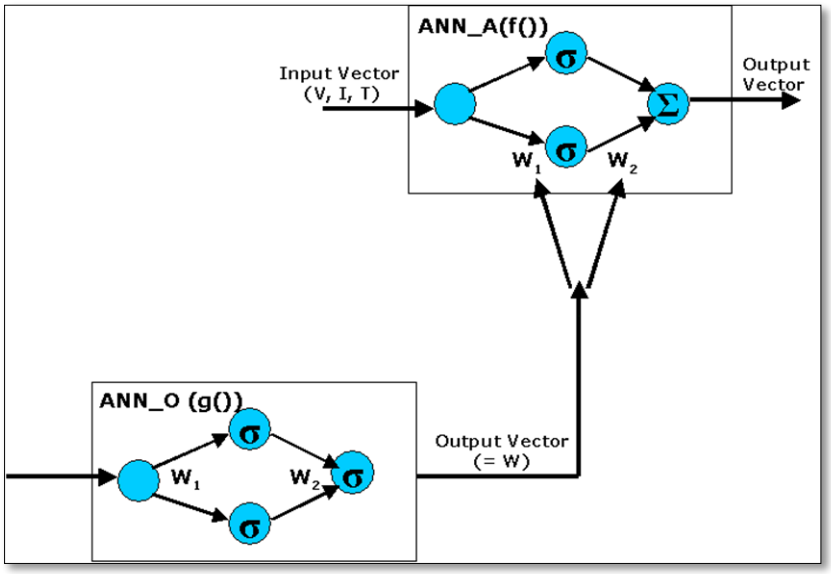


**Figure I.6 :** *Schematic Representation of Smart Battery Management using ANN [15].*

[16] presents a method of SOC determination suitable for mobile communication applications. The effects of pulse current loads are investigated using a three-layer feed-forward artificial neural network, which is trained using the back-propagation algorithm (for adjusting the weights and biases of each neuron on the basis of the error between SOC and the network's output). The paper shows the use of artificial neural networks to classify Li-ion battery discharge patterns under pulsed charges typical of those provided by the mobile telecommunications system.

In [17] SOC and SOH prediction based on fuzzy logic modelling is demonstrated for two battery systems, lithium–Sulphur dioxide and NiMH. The technique entails the use of fuzzy logic arithmetic to analyses statistics acquired by impedance spectroscopy and/or Coulomb counting techniques. Data can also be classified by way of 'crisp' or 'fuzzy' sets. Crisp units' categories records with certainty, e.g. a set of temperatures between 30°C and 40°C. With fuzzy sets, the set-in which information can be categorized is uncertain, e.g. the temperature is 'warm'. This linguistic descriptor 'warm' is a subset of a set of all temperatures and is described with the aid of its membership

function. The degree to which an element of the 'temperature' set belongs to the fuzzy subset 'warm' is indicated by way of a volume referred to as its 'degree of membership' or suit fuzzy unit value.

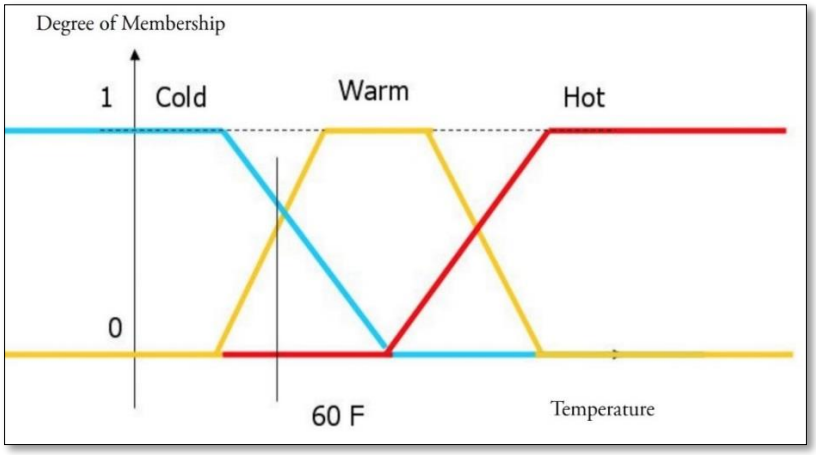


**Figure I.7:** *Temperature Adhesion Feature [17].*

Fig. I.7 indicates an example of three subsets, defined through their membership functions, 'cold', 'warm' and 'hot', of the 'universe of discourse' 'temperature' set. Using the above approach for a restricted record set the most error between the measured SOC and the model-predicted SOC received for li–Sulphur dioxide cells used to be observed to be +/– 5%.

- The SOC indication techniques are summarized in Table I.1 alongside with their fields of application.

**Table I.**1 **:** *Overview of Methods for SOC Determination [18].*

| Technique | Field of application | Advantages | Drawbacks |
|---|---|---|---|
| Discharge test | Used for capacity determination at the beginning of life | Easy and accurate; independent of SOH | Offline, time- intensive, modifies the battery state, loss of energy |
| Coulomb counting | All battery systems, most applications | Accurate if enough re-calibration points are available | Sensitive to parasite reactions |
| OCV | Lead, Lithium. | Online, cheap. | Needs long rest time |
| EMF | Lead, Lithium | Online, cheap, | Needs long rest time |
| Linear model | Lead Photovoltaic | Online, easy | Needs reference data for fitting parameters |
| Impedance spectroscopy | All systems | Gives information on SOH and quality | Temperature sensitive, cost intensive |
| D. C. Internal resistance | Lead, NiCd | Gives information on SOH; possibility of online measurements | Good accuracy, but only for a short time interval |
| Artificial Neural Networks | All battery systems | Online | Needs training data of a similar battery |
| Fuzzy logic | All battery | Online | Ask a lot of memory in real-word |
| Kalman filters | All battery systems, PV | Online Dynamic | Difficult to implement the filtering algorithm that considers all features as e.g. nonnormalities |

## I.5. Conclusions

This chapter gives an overview of the state-of - the-art of state-of-charge indication of rechargeable batteries, including a historical SOC technology. Where we see after this study that we will choose the coulomb counting method to study in the next chapters because it is the easiest and most effective method according to the approved references in this study.

# Chapter II:

# Battery Modeling

## II.1. Introduction

In this chapter we will learn about how batteries are charged and their models. We'll discuss the various types of batteries and their benefits and disadvantages. And we're going to look at the best form of battery today for your EV conversion, where we're going to talk intensively about the lithium and lead acid batteries in this chapter and then we're going to do specific research on these two types.

## II.2. Electric Vehicle Battery Technologies

### II.2.1. **Overview**

EV's chassis included mechanical elements, and its electrical motors and controllers. Its batteries will take you into the chemical zone now. Although there are all sorts of battery innovations going on in the laboratories, the aim here is to give you a brief history to the battery and introduce the lead-acid and lithium batteries with which you will be working on your EV conversion.

EV battery pack-a collection of 16 to 24 6-volt (or 12-volt equivalent) individual lead-acid and lithium batteries represents the single largest replacement cost item, and quite possibly is also your largest initial expense item, it’s worth spending some time learning about batteries so you can choose and use them wisely [20].

Batteries are the breath of your EV's life, and they should be familiar to any EV converter on three levels. To be battery graduate you need to:

- Comprehend what happens inside a battery
- Become familiar with the external properties of a battery
- Know the pros and cons of real-world batteries working

Knowledge in these three fields is a good investment in business and can save you time and money.

### II.2.2. **Basics of Lead Acid Battery**

Lead acid batteries have been around for more than a century. In the fully charged state, a 2V electric potential exists between the cathode and the anode [21]. Electrons are pushed through the load externally during discharge, while internal chemical reactions at the electrolyte interface and the electrodes work to balance the balance of charge. The chemical state of a fully charged and discharged lead acid battery is demonstrated in table II.1.

**Table II.1:** *Lead Acid Charge States [22].*

| | **Anode** | **Electrolyte** | **Cathode** |
|---|---|---|---|
| Fully Charged | $Pb$ | $H_2SO_4$ | $PbO_2$ |
| Fully Discharged | $PbSO_4$ | $H_2SO_4$ | $PbSO_4$ |

Lead acid batteries can be divided into two distinct categories: flooded and sealed/valve regulated (SLA or VRLA) [22]. The two types are similar in their internal chemistry (shown in Table II.1), and the device level design criteria are the most important variations between the two types. Flooded batteries with lead acid need three things VRLA doesn't:

1. Upright orientation against leakage of electrolytes.
2. Ventilated area, created during cycling to disperse the gasses.
3. Routine Electrolyte management.

Such variations include balancing the lower cost of flooded lead acid against the additional expense and secondary costs. There are two types of VRLA batteries: Gel and Absorbed Glass Mat (AGM). The different names represent different methods of electrolyte-containment. A thickening agent is inserted into Gel batteries to transform the electrolyte from liquid to gel. In AGM cells the liquid electrolyte is covered by a glass matrix.

"Deep cycle" and "shallow cycle" lead acid batteries can be found in both the VRLA and flooded classes. Shallow cycle VRLA batteries are commonly used for automotive start, light, ignition ("SLI") batteries that must deliver high power pulses for short durations [23]. The stationary power market uses a deep loop, as the batteries often discharge at a low rate over multiple hours.

### II.2.3. **Basics of Lithium-ion Battery**

The concept of a lithium-ion battery was initially conceived in the 1970's and began to see widespread adoption by the 1990's [21]. The basic mechanism is that a charged lithium ion is shuttled back and forth between the cathode and the anode during charge and discharge. Figure II.1 shows a diagram of a $LiCoO_2$ variation of the lithium-ion family.

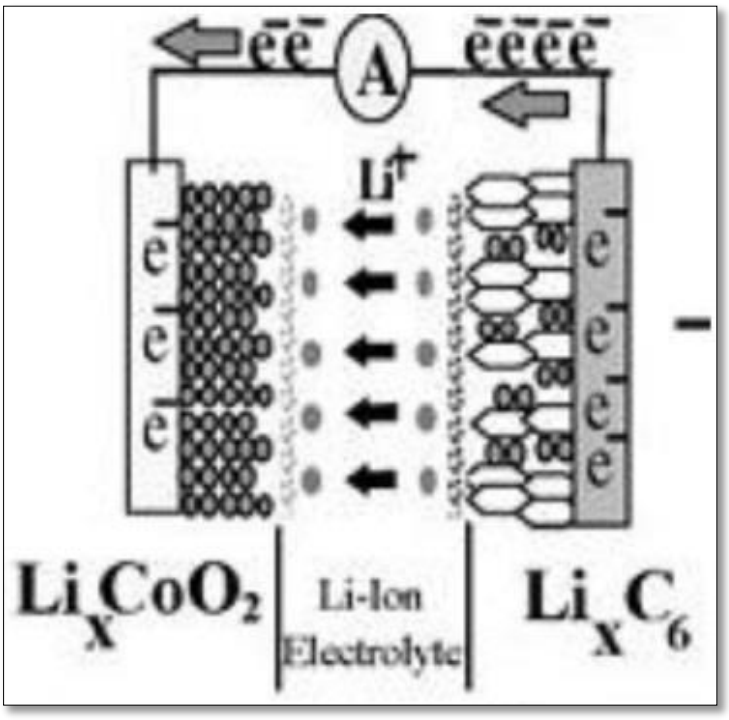


**Figure II.1:** *Lithium-ion Reaction [24].*

Chemical variations in the cathode, anode and electrolyte affect the efficiency of the cells, as do packaging geometry. The cathode chemistry is the factor most commonly altered from cell manufacturer to cell manufacturer with terms like LFP, NCM, NCA, Cobalt, and Manganese reflecting the cathode chemistry class [24]. Graphite constitutes over 90 percent of lithium-ion anodes; silicon and titanium-based materials are sometimes used to enhance life and efficiency, in return for substantially higher costs.

The electrolyte exists in liquid form, but for "lithium polymer" cells, the electrolyte is absorbed in a polymer membrane [25]. This allows cell manufacturers to use a pocket enclosure on the cell rather than the metal enclosure used when the liquid electrolyte in cylindrical and prismatic cells is present. Growing of those variations influences a lithium-ion cell's efficiency.

In spite of the various chemical variations, lithium-ion batteries can generally be separated into two groups: lithium iron phosphate (LFP, $LiFePO_4$) and metal oxides (NCM, NCA, Cobalt, Manganese) [26]. Table II.2 outlines the variations on a cell-level between the two chemical groups. The table values represent the average values provided that there are differences in each class.

**Table II.2:** *Lithium-ion Subcategory Comparison [27, 28].*

| | LFP | LiNCM |
|---|---|---|
| Voltage | 3.3 V nominal (2-3.6 V/cell) | 3.7 V nominal (2.7-4.2 V/cell) |
| Energy Density | 300 Wh/L | 735 Wh/L |
| Specific Energy | 128 Wh/kg | 256 Wh/kg |
| Power | 1000 W/kg | 512 W/kg |
| Cycle Life | 2,000 @ 100% DoD<br>3,000 @ 80% DoD | 750 @ 100% DoD<br>1,900 @ 80% DoD |
| Calendar Life | 6 years | 8 years |
| Max recommended temperature | 40°C | 55°C |
| Safety | High | Moderate |
| Commercial Suppliers | A123, Valence, BAK, BYD, K2, Lishen, many Chinese vendors | Sanyo, Panasonic, Samsung, DowKokam, Sony, LG Chem, Moli |

Both lithium-ion cells are "deep cycle" which means they are capable of being both charged and discharged. The battery life would improve dramatically if increasing discharge depth is limited to 80 per cent of the rated capacity.

## II.3. Methods of Charging Electric Vehicle Battery

### II.3.1. Methods of Charging Lead-Acid Batteries

#### a) Taper Charging Method

Taper charging is a variation of the modified constant-potential method, using less sophisticated controls to reduce equipment cost. This method does result in gassing at the critical point of recharge, and the cell temperature is increased [29].

The end of the charge is often controlled by a fixed voltage rather than a fixed current. Therefore, when a new battery has a high counter- EMF, this final charge rate is low and the battery often does not receive sufficient charge within the time period allotted to maintain the optimum charge state [29]. In the latter part of life when the counter-EMF is small, the charging rate is higher than the usual finishing rate and thus the battery receives excessive charging, which degrades life.

For photovoltaic battery systems and other systems designed for maximum life, circuits for charging and regulating will generate a voltage and current pattern equal to the best industrial circuits. Changed constant-potential charging methods are favored with starting constant current. Optimum control to maximize the life and energy output from the battery is best achieved when the depth of discharge and the time for recharge are predetermined and repetitive, a condition which is not always realized in solar photovoltaic applications [30].

b) **Float Charging Method**

Float charging is a low-rate, constant-potential charging and is often used to hold the battery fully charged. This method is primarily employed for stationary batteries that can be charged from a DC bus. The float voltage for a non-antimonial grid battery containing 1.210 specific gravity electrolytes and have an open-circuit voltage of 2.059 V per cell is 2.17 to 2.25 V per cell [30].

### II.3.2. **Methods of Charging Lithium Batteries**

a) **Five-step Charging Pattern**

As seen in the CC-CV method above, the CV stage prolongs the charging time and reduces the cycle life of the battery. For that reason, an alternative method is derived in order to reduce the charge time and give more life cycles for the cell. The five-step charging method consists of partitioning the charging time into 5 steps [31]. In each step, the battery is charged with a different and lower constant current for some duration shown in Fig. II.2 While charging, the battery voltage increases until it reaches a preset value, at this moment the charger switches to the next step. The charging current in each step is set to predetermined value; this value is found in different algorithms [32, 33]. In this step a Particle Swarm Optimization (PSO) based search method will be mentioned.

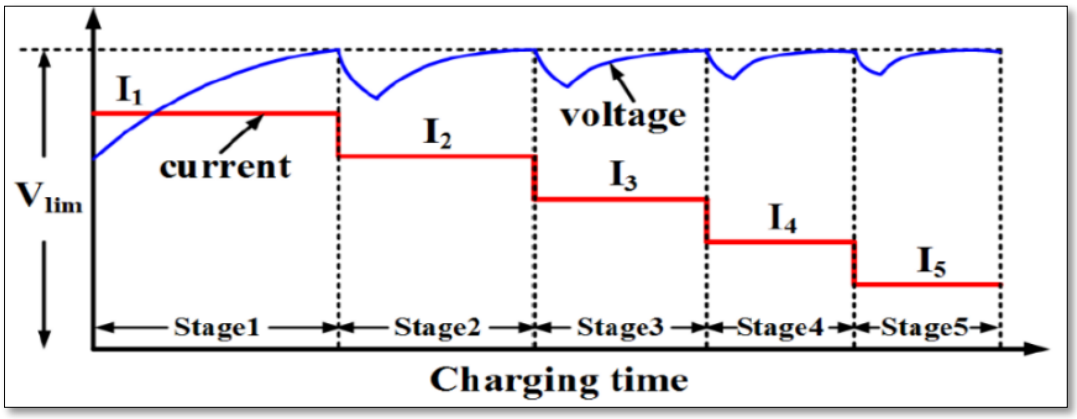


**Figure II.2:** *Five-step Charging Pattern [32].*

One way of achieving the optimum charging pattern is by using the PSO technique. The PSO is an evolutionary computational technique focused on the population and inspired by the social behavior of bird flocks. It has attracted many researchers for its simplicity in implementation where it has few parameters to tune and adjust, features the characteristic of fast convergence and less computational time, non-gradient derivative-free algorithm which can estimate several solutions in a single iteration, there is no relation between the solution obtained and the initial solution [32]. A PSO is composed of several particles, which form a swarm, moving in the feasible solution space in search of the optimal solution shown in Fig II.3. Each particle will exchange information with the rest of the swarm in order to find the global best solution ($G_{best}$). In each iteration, every particle will update its flying direction based on its own best solution ($P_{best}$) and ($G_{best}$) according to the model equations as follows:

$$\boldsymbol{v_{id}^{k+1} = wv_{id}^{k} + C_1 rand_1^k\left(Pbest_{id}^{k} - x_{id}^{k}\right) + C_2 rand_2^k\left(Gbest_{d}^{k} - x_{id}^{k}\right)} \quad \textbf{(II.1)}$$

$$\boldsymbol{x_{id}^{k+1} = x_{id}^{k} + v_{id}^{k+1}} \quad \textbf{(II.2)}$$

where, $v_{id}^{k}$ is the value of dimension $d$ in the velocity vector of particle $i$ at iteration $k$. $x_{id}^{k}$ is the position of particle $i$ along dimension $d$ at iteration $k$. $w$ is the selected inertia weight, $C_1$ and $C_2$ are the cognitive and social learning rates, respectively, which change the velocity of a particle towards $P_{best}$ and $G_{best}$.

To find the optimum five-step charging speeds for C to satisfy the quick charging requirements and the best cost benefits for charging, the PSO algorithm is used to find the optimum charging pattern. The formulation of problems is defined as follows:

Maximize $$\boldsymbol{f_{cost}^{i}\left(T_{ch}^{i}, C_{dis}^{i}\right) = \alpha T_{ch}^{i}\left(\vec{I}_j^{\,i}\right) + \beta C_{dis}^{i}\left(\vec{I}_j^{\,i}\right), \qquad \vec{I}_j^{\,i} \in \mathbb{S}} \quad \textbf{(II.3)}$$

Where, $$\vec{I}_j^i = [\, I_1^i, I_2^i, I_3^i, I_4^i, I_5^i \,]$$

Subject to: $$\mathbf{30} \leq T_{ch}^i\left(\vec{I}_j^i\right) \leq \mathbf{90}\ \boldsymbol{min}$$

$$\mathbf{80\%} \leq C_{dis}^i\left(\vec{I}_j^i\right) \leq \mathbf{100\%}$$

$$I_j^i \geq I_k^i \text{ if } j < k, \quad j, k = 1, 2, \ldots, 5$$

Where, $f_{cost}^i$ is the cost function for battery $i$ (particle $i$) which is a function of charging time ($T_{ch}^i$) and discharge capacity ( i ) dis C and both are dependent of the current value of the five stage pattern. S is the set of all feasible solution. α, β are weightings used to highlight the impact of each parameter on the cost function. These weightings are found in [32] using fuzzy logic control to obtain the best fitness evaluation.

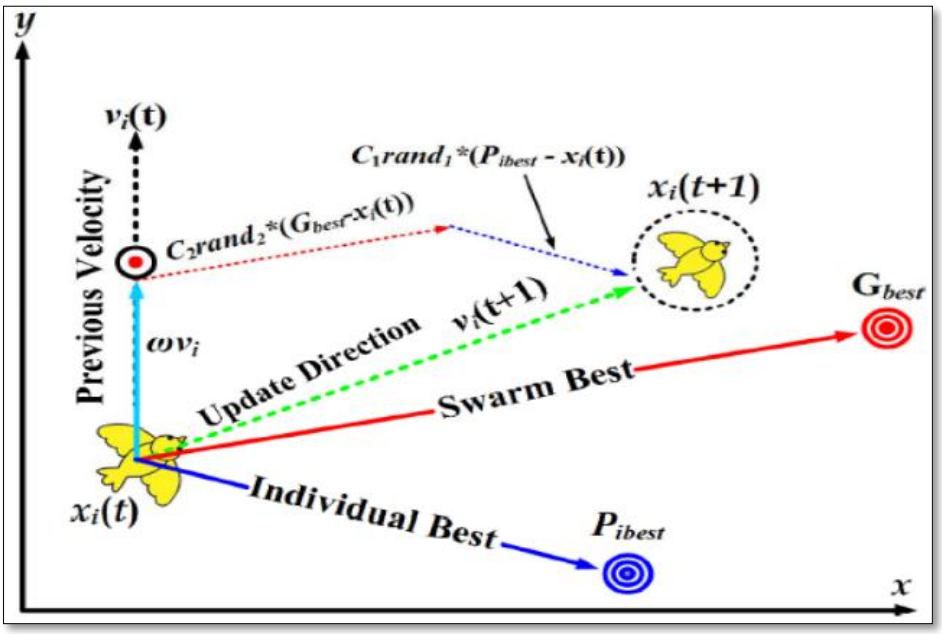


**Figure II.3:** *PSO Updating Concept [32].*

b) **Boost Charging Method**

Although electronic devices are becoming increasingly important in the everyday lives of individuals, the need for a quick charging method has become a requirement. The charging times are long with normal charging methods such as CC-CV methods due to safety conditions and cycle life requirements. Today the reality is unacceptable. Therefore, a charging method called "boost charging" is known as an ultra-fast charging method for Li-ion batteries, through

which batteries can be recharged with very high current for a limited period of time close to fully discharged. The detrimental effect of charging the battery with high current is taken into consideration so that the boost charge method does not introduce any negative degradation effects [34].

### II.3.3. **Common Methods to Charge the Batteries**

#### a) **Constant-Current Charging**

Constant-current recharging is not commonly used for lead-acid batteries but for lithium batteries at one or more current speeds. This is due to the need for current adjustment unless the charge current is kept at low during the charge (Ampere-hour rule), resulting in long charge times of 12 h or more. Typical charger and characteristics of the battery for continuous current charging, for single and two-stage charging. Some small lead-acid batteries use constant-current charging. Due to the ease of measuring Ampere-hour input and since constant-current charging can be achieved with easy, inexpensive equipment, constant-current charging is also sometimes used in the laboratory. In the field, constant-current charging at half the 20-h rate can be used to decrease sulfating in overloaded or underloaded batteries. This treatment, however, may diminish the battery life and should be only used with the advice of the battery manufacturer [30].

#### b) **Constant-Potential Charging**

The modified constant-potential charging methods (methods b and c) are used in typical industrial applications. Modified constant charging capacity is used for on - the-road vehicles and applications for electricity, telecommunications and uninterruptible power systems where the charging circuit is connected to the battery. The charging circuit has a current limit in this case, and that value is retained until a fixed voltage is reached. The voltage is then kept constant until the battery is asked to discharge. Decisions on the current limit and the constant-voltage value must be made. This is determined by the time period when the battery is at constant voltage at a charge state of 100 per cent. A low charge current is desirable to reduce overload, grid corrosion associated with overload, water loss due to electrolysis of the electrolyte, and maintenance to substitute this water for this "float'-type operation with the battery still on load. Achieving a full recharge with a low constant potential requires the proper selection of the starting current, which is based on the manufacturer’s specifications [35].

The adjusted constant-potential charge, with constant start and finish levels, is normal for deep-cycling batteries typically discharged at a depth of 80 percent at the 6-h rate; recharging is usually completed in an 8-h cycle. The charger is set for the constant potential of 2.39 V per cell (the gassing voltage), and the starting current is limited to 16 to 20A per 100 Ah of the maximum 6-h Ampere-hour range by means of a series of charger circuit resistors. This initial current remains constant until the battery's average cell voltage exceeds 2.39 V. At constant voltage, the current decays to the finishing rate of 4.5 to 5A per 100 Ah, which is then sustained until the end of the charge. A Timer monitors the total charge time. The time of charge is selected to ensure a recharge input capacity of a predetermined percent of the Ampere-hour output of the previous discharge, normally 110 to 120%, or 10 to 20% overcharge. The 8-h charging time can be reduced by increasing the initial current limit rate [30].

c) **Pulse Charging**

This method aims at obtaining an even distribution of ions in the battery electrolyte, speeding up the charging process, and slowing battery polarization and increasing life cycles.

The charging frequency is critical in this form of loading process. It relates to the time and efficiency of charging. Different techniques are being carried out to determine the optimal charging frequency instead of the outdated techniques of trial and error. It has suggested the varied duty pulse charge, it can detect the best pulse charging duty cycle to get the best charging speed and output. The AC impedance technique is suggested to find the optimal pulse charging frequency related to the minimum AC impedance frequency [36, 37].

The duty varied pulse charge strategy consists of changing the duty cycle. It is based on the fact that a smaller duty cycle, $D$, means better current density exchange $i_0$ which results with better efficiency and with larger rest period the charging time will be long. Therefore, it is important to compromise between high charging efficiency and faster battery charge. Thus, the pulse charge factor is defined as:

$$\boldsymbol{\eta = D.i_0} \tag{II.4}$$

Given that, the exchange current density $i_0$ is given by:

$$\boldsymbol{i_0 = Fk_0(1-\theta)^{1-\alpha}\theta^{\alpha}c^{1-\alpha}} \tag{II.5}$$

The pulse charge factor will be as follow:

$$\boldsymbol{\eta = D.F.k_0(1-\theta)^{1-\alpha}\theta^{\alpha}c^{1-\alpha}} \tag{II.6}$$

It is necessary to note that α and c are not proportional to (1-D), so the service cycle D is not set at 50 per cent for better efficiency and quick charge time. Thus, a search method is implemented into the controller to find the best load duty cycle that results in the best pulse charge factor.

Concerning the optimal pulse charge frequency, the AC impedance technique is widely used [38, 39]. The AC impedance model of the Li-ion battery given in Fig. II.4 is formed by, ohmic resistance, $R_0$, charging transfer resistance, $R_{ct}$, Warburg impedance, $Z_w$, a capacitance, $C_d$, and an electrode inductance, $L_d$,. Different charging frequency can charge the AC impedance of the battery, therefore, to obtain the minimum loss in the battery impedance and maximum charging energy the pulse charging frequency is set to be equal to the minimum AC impedance frequency $f_{z_{min}}$.

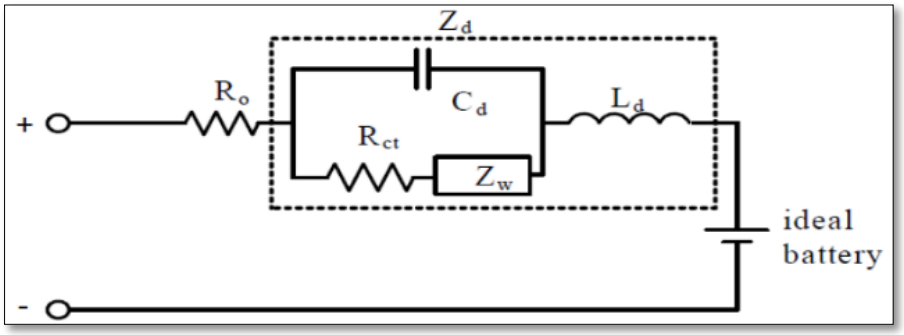


**Figure II.4:** *AC Impedance Model [7].*

## II.4. Types of Battery Models

### II.4.1. Lead Acid Battery Models

Modeling of the lead acid batteries can be done in numerous ways depending on the system requirement and accuracy [40]. These include Electrochemical Models, Models of Computational Fluid Dynamics, Models of Finite Elements and Models of Electric Equivalents. Such models involve experimentation to determine battery characteristics and plot response curves, measuring voltage and currents during charging and discharging phase. Electrochemical Models, Computational Fluid Dynamics Models, Finite Element Models are effective in acquiring battery technological knowledge but not very useful in actual simulation and device behavior analysis. But the electrical equivalent circuit model describes the various parameters and characteristics of the battery via the electrical equation, which is useful for the purpose of simulation which device behavior analysis.

Studying the various models goes from a very basic battery model to a complicated battery model. The research is conducted to obtain in-depth knowledge of the battery's electrical behavior. Thus, various models of electrical batteries are listed below:

**a) Simple Battery Model**

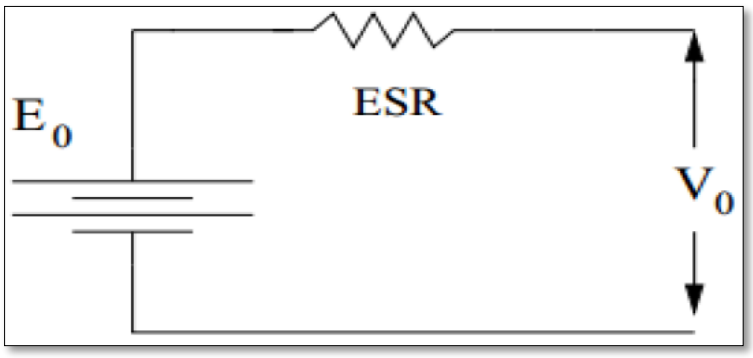


**Figure II.5:** *Equivalent Circuit of Simple Model [41].*

If battery was linear then it acts as an electric bipolar. A simple ideal model consists of $E_0$ as the electromotive force of the battery and a constant equivalent resistor ESR connected in series as an internal resistance. $V_0$ is the terminal voltage of the battery [41]. $V_0$ can be obtained by measuring the open circuit voltage and ESR can be obtained from both open circuit measurement and with load connected when the battery is fully charged

**b) Thevenin Battery Model**

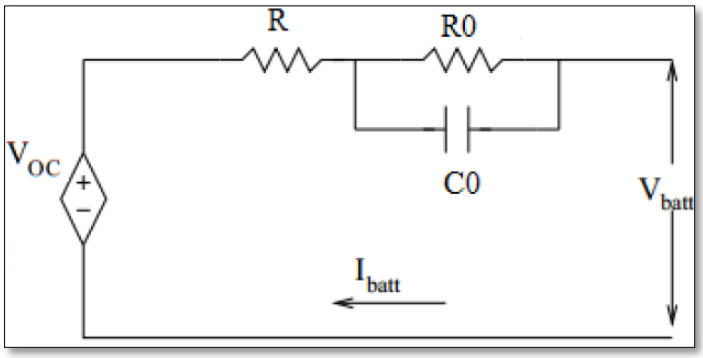


**Figure II.6:** *Equivalent Circuit of Thevenin Model [42].*

Thevenin battery model is one of the most commonly used battery models. The model consists of ideal no-load battery voltage $V_{oc}$, internal resistance (R), Capacitance ($C_0$) and over voltage resistance ($R_0$). Capacitance between electrolyte and electrodes is given by ($C_0$)

whereas $R_0$ represents the battery overvoltage due to the contact resistance of plate to electrolyte [42].

$$\boldsymbol{V_{batt} = V_{oc} - (I_{batt}R - V_0)} \quad \textbf{(II.7)}$$

$$\boldsymbol{V_0 = \left(\frac{1}{R_0} + \frac{1}{C_0}\right) I_{batt}} \quad \textbf{(II.8)}$$

c) **Copetti Model**

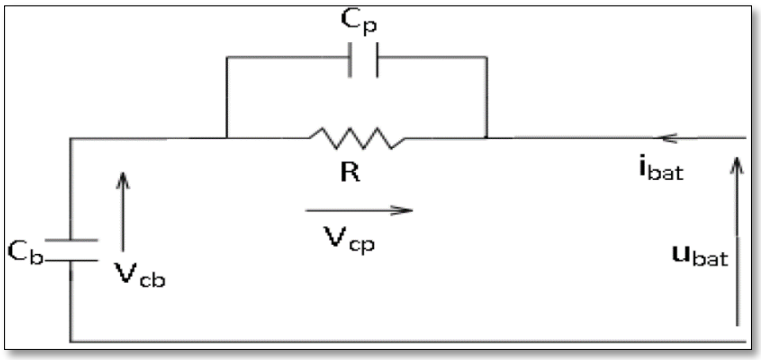


**Figure II.7:** *Equivalent Circuit of Copetti Model [43].*

The model is a generic battery model that has constant parameters and is valid for any battery size. This model is simple, since it does not require the experimental identification of empirical parameters. The model is defined according to the following equation:

If $u_{batt} < nV_g$

$$\boldsymbol{u_{batt} = n\left(V_{cb}(t) + V_{cp}(t)\right)} \quad \textbf{(II.9)}$$

$$\boldsymbol{\frac{dV_{cb}}{dt} = \frac{i_{bat}(t)}{C_b(t)}} \quad \textbf{(II.10)}$$

$$\boldsymbol{\frac{dV_{cp}}{dt} = -\frac{1}{R(t)C_p}V_{cp} + \frac{i_{bat}(t)}{C_p}} \quad \textbf{(II.11)}$$

If $u_{batt} > nV_g$

$$\boldsymbol{u_{batt}(t) = n\left(V_{cb}(t) + R(t)i_{bat}(t)\right)} \quad \textbf{(II.12)}$$

$$\boldsymbol{SOC(t) = 1}$$

### II.4.2. **Lithium Battery Models**

#### a) **Equivalent Circuit Model**

The analogous circuit model can be used for simulating the battery's complex properties. It's composed of circuit elements such as resistors, condensers, a source of constant voltage, ... It can be used for the different battery working conditions, and the model's state-space equations can be deduced to enable study and application. This model is also commonly used in modelling simulations and battery management systems for different types of electric vehicles.

The Rint model in Figure II.8, designed by the Idaho National Laboratory, uses an ideal voltage source to describe the open-circuit voltage of the battery. The battery's internal resistance $R$ and the open-circuit voltage are functions of the SOC and temperature, and the internal resistance value changes when charging under the same SOC [44].

In Figure II.9, the Thevenin model, which is the most typical circuit model, considers the characteristics of the battery as capacitive and resistive. The model uses an ideal voltage source $U_{ocv}$ to describe the open-circuit voltage of the battery, and the resistance $R_\Omega$ is the ohmic resistance of the battery, while the capacitor and resistor are connected in parallel in order to describe the battery's over-potential [45].

The RC model in Figure II.9, which consists of two capacitances and three resistances, is designed by the famous battery manufacturer SAFT. The large capacitance $C_B$ describes the energy storage capacity; the small capacitance $C_C$ describes surface effects of the battery electrodes; the resistance $R_T$ is referred to as the terminal resistance;

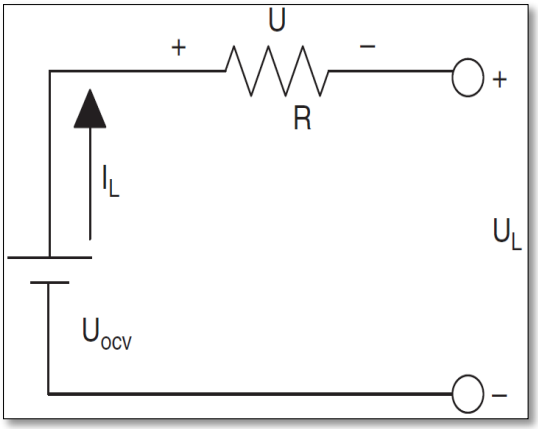


**Figure II.8:** *Circuit Structure of Rint Model [44].*

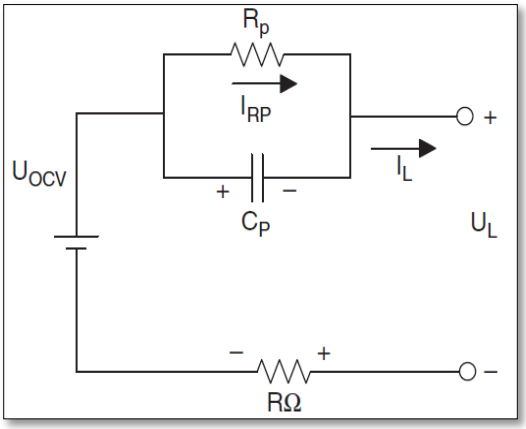


**Figure II.9:** *Circuit Structure of Thevenin Model [45].*

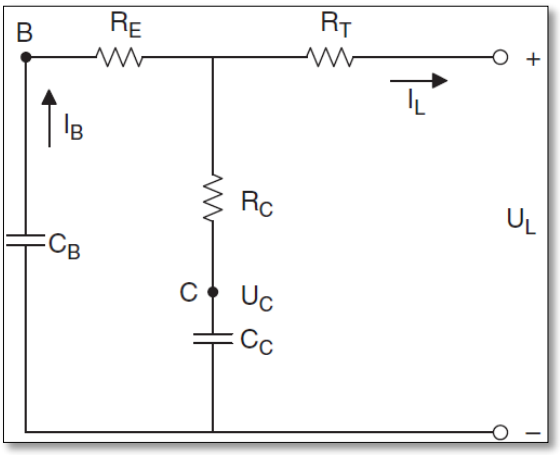


**Figure II.10:** *Circuit Structure of RC Model [46].*

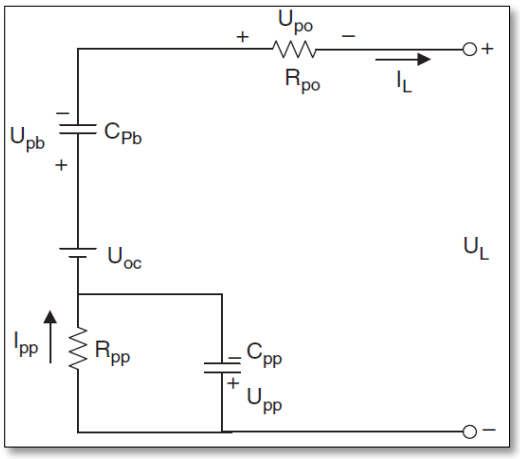


**Figure II.11:** *Circuit Structure of PNGV Model [46].*

as the cut-off resistance; and the resistance $R_C$ is referred to as the capacitive resistance. In this model, the cathode of the battery is defined as the zero-potential point.

The PNGV model in Figure II.10 is the standard battery model in the "PNGV Battery Test Manual" in 2001, and extended into the standard battery model in "Freedom CAR Battery Test Manual" in 2003. In this model, $U_{OC}$ is an ideal voltage resource, indicating open-circuit voltage of a battery, $R_{PO}$ is the ohmic internal resistance, $R_{PP}$ the polarization internal resistance, $C_{PP}$ the polarization capacitance, $I_{PP}$ the current with respect to polarization resistance; the capacitance $C_{Pb}$ describes the cumulative open-circuit voltage change with respect to loading time [46].

b) **Electrochemical Model**

The electrochemical model uses mathematical methods to describe the internal reaction process of a battery, based on electrochemical theory [24]. The Peukert formula is the most typical battery model, seen in Equation II.13, which expresses that the available charging of a battery decreases with increasing discharging current.

$$\boldsymbol{I^n T_i = Constant} \qquad \textbf{(II.13)}$$

where *I* is the discharging current, n the constant of a battery, and $T_i$ is the discharging time under current *I*.

The Shepherd model was proposed in 1965 and is expressed as Equation II.13. Electro-chemical activities are described by the voltage and current of a battery [24].

$$E_t = E_O - R_i - K_i\left(\frac{1}{1-f}\right) \quad \textbf{(II.14)}$$

where $E_t$ is the terminal voltage of a battery, $E_O$ the open-circuit voltage of a fully charged battery, $R_i$ the ohmic internal resistance, $K_i$ the polarization resistance, $I$ the transient current and $f$ the net discharging capacity calculated according to the Ah integration method. The Shepherd model is commonly used to analyze hybrid cars, and to calculate battery voltage and SOC together with the Peukert equation under different powers.

The Shepherd model applies to a small constant current battery and is able to find the turning point where the terminal voltage begins to rapidly decrease. Such a critical state happens occasionally during an electric car battery's actual operating cycle. In Equations II.14–II.16, Unnewehr and Nasar simplified the Shepherd model;

$$E_t = E_O - R_i - K_i f \quad \textbf{(II.15)}$$

$$E_{OC} = E_O - K_i f \quad \textbf{(II.16)}$$

$$R = R_O - K_R f \quad \textbf{(II.17)}$$

where $E_{OC}$ is the open-circuit voltage, $R_O$ the total internal resistance of a fully charged battery, $K_R$ the experimental constant, and $R$ the battery equivalent resistance.

It is developed into the Nerst model and the Nerst expanded model based on the Unnewehr model, respectively expressed in Equations II.16 and II.18.

$$E_t = E_i - R_i I - K_i \ln(f) \quad \textbf{(II.18)}$$

$$E_t = E_O - R_i I - K_i \ln(f) + K_j \ln(1\_f) \quad \textbf{(II.19)}$$

Based on the Shepherd model, the Unnewehr model and the Nerst expanded model, Dr. Gregory L. Plett from Colorado University developed a group formulation of the above three electrochemical models, seen in Equation II.19.

$$U_L = K_O - RI_L - \frac{K_1}{SOC} - K_2 SOC + K_3 \ln(SOC) + K_4 \ln(1 - SOC) \quad \textbf{(II.20)}$$

where UL is the battery loading voltage, IL the current, R the battery internal resistance, and K0, K1, K2, K3, and K4 are the mean model coefficients, respectively.

c) **The Fractional-Order Model**

Figure II.12 demonstrates the electrochemical impedance spectroscopy (EIS) test results for the battery 1-cell 2 [47]. There is a semicircle in the middle-frequency spectrum

whose center is under the horizontal axis. In general, this phenomenon is known to be connected to the double layer at the electrode-electrolyte interface.

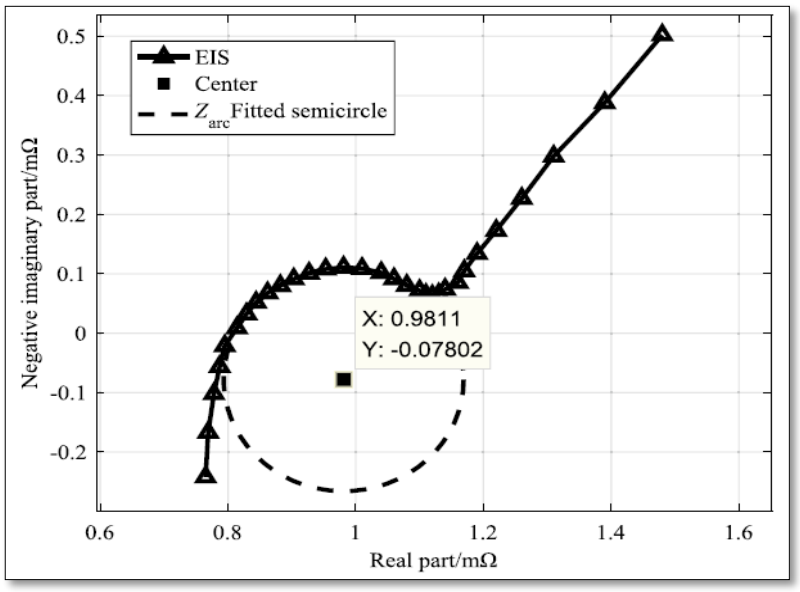


**Figure II.12:** *The Dispersion Effect in Electrochemical Impedance Spectroscopy [47].*

The researchers discovered when fitting impedance spectra that the ECM frequently failed to achieve the desired fitting precision using ideal capacitances. The phenomenon that the double layer's calculated frequency response characteristics are incoherent with the pure capacitance is called the dispersion impact. This deviation from the pure capacitance can be fitted by a ***constant phase element (CPE)***. Its impedance expression is as follows [48]:

$$\boldsymbol{Z'_{CPE}(\omega) = \frac{\omega^{-\alpha}}{Y}\cos\left(\frac{\alpha\pi}{2}\right), Z'_{CPE}(\omega) = \frac{\omega^{-\alpha}}{Y}\sin\left(\frac{\alpha\pi}{2}\right), 0 < \alpha < 1} \quad \textbf{(II.21)}$$

where $\omega$ indicates the angular frequency. The CPE has two parameters. The first parameter is $Y$, with its unit being $s^n\Omega^{-1}$. The second parameter, $\alpha$, is a dimensionless exponent which is used to measure how far the CPE deviates from the pure capacitor element. If $\alpha = 0$, the CPE is a pure resistance element. If $\alpha = 1$, it converts into a pure capacitance element.

It can be seen from Eq. (II.22) that the phase angle of the CPE satisfies

$$\boldsymbol{\tan\phi = \tan\left(\frac{\alpha\pi}{2}\right), \phi = \frac{\alpha\pi}{2}} \quad \textbf{(II.22)}$$

Therefore, the phase angle of the element is the independent of frequency, for which it is known as the constant phase angle element.

In the impedance spectra fitting, the CPE is often used in parallel with a pure resistance, and its impedance is recorded as $Z_{arc}$. It is expressed as:

$$\boldsymbol{Z^0_{arc}(\omega) = \frac{\frac{1}{R} + Y\omega^{\alpha}\cos\left(\frac{\alpha\pi}{2}\right) - jY\omega^{\alpha}\sin\left(\frac{\alpha\pi}{2}\right)}{\left(\frac{1}{R}\right)^2 + \left(\frac{2}{R}\right)Y\omega^{\alpha}\cos\left(\frac{\alpha\pi}{2}\right) + (Y\omega^{\alpha})^2}} \quad \textbf{(II.23)}$$

$$\boldsymbol{Z'_{arc}(\omega) = \frac{\frac{1}{R} + Y\omega^{\alpha}\cos\left(\frac{\alpha\pi}{2}\right)}{\left(\frac{1}{R}\right)^2 + \left(\frac{2}{R}\right)Y\omega^{\alpha}\cos\left(\frac{\alpha\pi}{2}\right) + (Y\omega^{\alpha})^2}} \quad \textbf{(II.24)}$$

$$\boldsymbol{Z''_{arc}(\omega) = \frac{-jY\omega^{\alpha}\sin\left(\frac{\alpha\pi}{2}\right)}{\left(\frac{1}{R}\right)^2 + \left(\frac{2}{R}\right)Y\omega^{\alpha}\cos\left(\frac{\alpha\pi}{2}\right) + (Y\omega^{\alpha})^2}} \quad \textbf{(II.25)}$$

By eliminating $Y$, we get:

$$\boldsymbol{\left(Z'_{arc}(\omega) - \frac{R}{2}\right)^2 + \left[Z''_{arc}(\omega) - \frac{R\cot\left(\frac{\alpha\pi}{2}\right)}{2}\right]^2 = \left[\frac{R}{2\sin\left(\frac{\alpha\pi}{2}\right)}\right]^2} \quad \textbf{(II.26)}$$

It is indicated that the arc of the intermediate frequency in Fig. II.12 can be fitted by the Eq. (II.25). The larger the parameter α is, the greater distance from the center of the arc to the real axis, which also proves that the pure capacitor ($\alpha = 1$) is incapable to fit the dispersion effect [49, 50].

However, the CPE is difficult to handle in the time domain and needs to be processed by fractional calculus theory. There are the following three commonly used definitions of fractional calculus [51]:

- ☒ The definition of Gruenwald–Letnikov (G-L) The G-L definition is derived from the traditional integer calculus and is defined as:

$$\boldsymbol{{}^0_aD^{\alpha}_t f(t) = \lim_{h\to 0} h^{-\alpha} \sum_{j=0}^{[(t-a)/h]} (-1)^j \binom{\alpha}{j} f(t-jh)} \quad \textbf{(II.27)}$$

The above formula is a unified expression of fractional differential and integral, where ${}^0_aD^{\alpha}_t$ indicates a fractional calculus operator. The positive and negative of $\alpha$ represent the fractional differential and integral, respectively. $a$ and $t$ denote the lower and upper limits of

calculus. $h$ is defined as the step size. $[(t-a)/h]$ presents the rounding up of $(t-a)/h$. $\binom{\alpha}{j}$ indicates the binomial coefficient:

$$\binom{\alpha}{j} = \begin{cases} 1 & j = 0 \\ \dfrac{\alpha(\alpha-1)\ldots(\alpha-(j-1))}{j!} & j > 0 \end{cases} \quad \textbf{(II.28)}$$

☒ The definition of Riemann–Liouville (R-L)

R-L integral definition:

$$ {}_{a}^{0}D_{t}^{-\alpha} f(t) = \frac{1}{\Gamma(-\alpha)} \int_{a}^{t} (t-\tau)^{-\alpha-1} f(\tau) d\tau \quad \textbf{(II.29)}$$

R-L differential definition:

$$ {}_{a}^{0}D_{t}^{\beta} f(t) = \frac{1}{\Gamma(n-\beta)} \frac{d^n}{dt^n} \left[ \int_{a}^{t} (t-\tau)^{n-\beta-1} f(\tau) d\tau \right] \quad \textbf{(II.30)}$$

where $0 < \alpha \leq 1,\ n-1 < \beta \leq n, n \in \mathbb{N}$.

☒ The definition of Caputo

Caputo integral definition:

$$ {}_{a}^{0}D_{t}^{-\alpha} f(t) = \frac{1}{\Gamma(-\alpha)} \int_{a}^{t} (t-\tau)^{-\alpha-1} f(\tau) d\tau \ \ (\alpha > 0) \quad \textbf{(II.31)}$$

Caputo differential definition:

$$ {}_{a}^{0}D_{t}^{\beta} f(t) = \frac{1}{\Gamma(n-\beta)} \int_{a}^{t} (t-\tau)^{n-\beta-1} f^{(n)}(\tau) d\tau \quad \textbf{(II.32)}$$

where $n-1 < \beta < n, n \in \mathbb{N}$.

It can be verified that G-L and R-L meanings are entirely identical to most functions. R-L concepts are used the most often in the theoretical research. Caputo definition is best suited to define and address initial value problems of fractional differential equations, while G-L definition offers the most direct form and method for approximating discretization.

## II.5. Comparing Lithium-ion and Lead Acid Batteries

Table II.3 presents a brief analysis of lithium-ion lead acid (LiNCM) at pack point. It should be remembered that there is a wide variety of parameter values in both chemistries, so this table is just a simplified representation of a very complex comparison.

**Table II.3:** *Battery Technology Comparison [29, 52, 53] .*

| | Flooded lead acid | VRLA lead acid | Lithium-ion (LiNCM) |
|---|---|---|---|
| Energy Density (Wh/L) | 80 | 100 | 250 |
| Specific Energy (Wh/kg) | 30 | 40 | 150 |
| Regular Maintenance | Yes | No | No |
| Initial Cost ($/kWh) | 65 | 120 | 600 |
| Cycle Life | 1,200 @ 50% | 1,000 @ 50% DoD | 1,900 @ 80% DoD |
| Typical state of charge window | 50% | 50% | 80% |
| Temperature sensitivity | Degrades significantly above 25°C | Degrades significantly above 25°C | Degrades significantly above 45°C |
| Efficiency | 100% @20-hr rate<br>80% @4-hr rate<br>60% @1-hr rate | 100% @20-hr rate<br>80% @4-hr rate<br>60% @1-hr rate | 100% @20-hr rate<br>99% @4-hr rate<br>92% @1-hr rate |

A significant observation of this table is that various standard charging windows have various chemistries. The consequence of this is that in order to have the same amount of energy available a lead acid battery will have a greater nameplate energy efficiency than the lithium-ion battery.

Given the major variations in the technological and economic characteristics of the types of batteries, it is fair that the "best" solution for which battery type is to be used is unique to application. Following is a closer look at some of the issues dealt with in Table II.3.

a) **Cycle Life Comparaison**

Lithium-ion has significantly higher cycle life than lead acid in deep discharge applications. The disparity is further increased as ambient temperatures increase. The cycle life of each chemistry can be increased by limiting the depth of discharge (DoD), discharge rate, and temperature, but lead acid is generally much more sensitive to each of these factors [54].

In hot climates where the average temperature is 92°F, the disparity between lithium-ion and lead acid is further exacerbated. The cycle life for lead acid (flooded and VRLA) drops to 50% of its moderate climate rating while lithium-ion will remain stable until temperatures routinely exceed 120°F [54].

b) **Rate Performance**

One important factor for lead acid is how long the device would take to discharge when deciding what battery capacity to use with a device. The shorter the discharge period, the less capacity is available from the lead acid battery. This condition makes lithium-ion very well suited for applications where full discharge occurs in less than eight hours [55].

c) **Cold Weather Performance**

Both lead acid and lithium-ion lose capacity in cold weather environments, but lithium-ion loses significantly less capacity as the temperature drops into the -20°C range [55]. The rate of discharge affects the output of lead acid, so two different values for the VRLA battery have been seen.

d) **Environmental Impact**

Concerning environmental friendliness, the lead acid batteries compete badly with the lithium-ion. In order to achieve the same energy storage, lead acid batteries need several times rawer material than lithium-ion, making a much greater effect on the environment during the mining process. The lead manufacturing industry is also extremely energy-intensive, resulting in significant quantities of contamination. While lead is highly hazardous to human health, the manufacturing methods and packaging of batteries make the risk to humans negligible. On the

plus side, over 97% of lead acid batteries in the United States are recycled, which makes a huge impact on the environmental equation [56].

Lithium is not without its own environmental problems [56]. Lithium carbonate, copper, aluminum, and iron ore are essential components of a lithium-ion battery. Furthermore, lithium mining is resource-intensive because lithium is only a small portion of the battery cell by mass, so the environmental effects of aluminum and copper are much greater. Right now, the lithium-ion recycling industry is still in its infancy, but the cell materials have demonstrated a high recovery and recyclability potential, and lithium-ion recycling levels are expected to exceed lead acid.

e) **Safety**

Lead acid and lithium-ion cells are capable of undergoing "thermal runaway" where the cell heats up rapidly and can release electrolyte, flames and toxic fumes. For lithium-ion, the probability and effects of an occurrence are greater, since it has a larger amount of energy in a smaller volume. Multiple cell and pack safety precautions shown in Figure II.13 are taken to prevent trigger events, such as short circuits and overheating, but incidents still occur[57] .

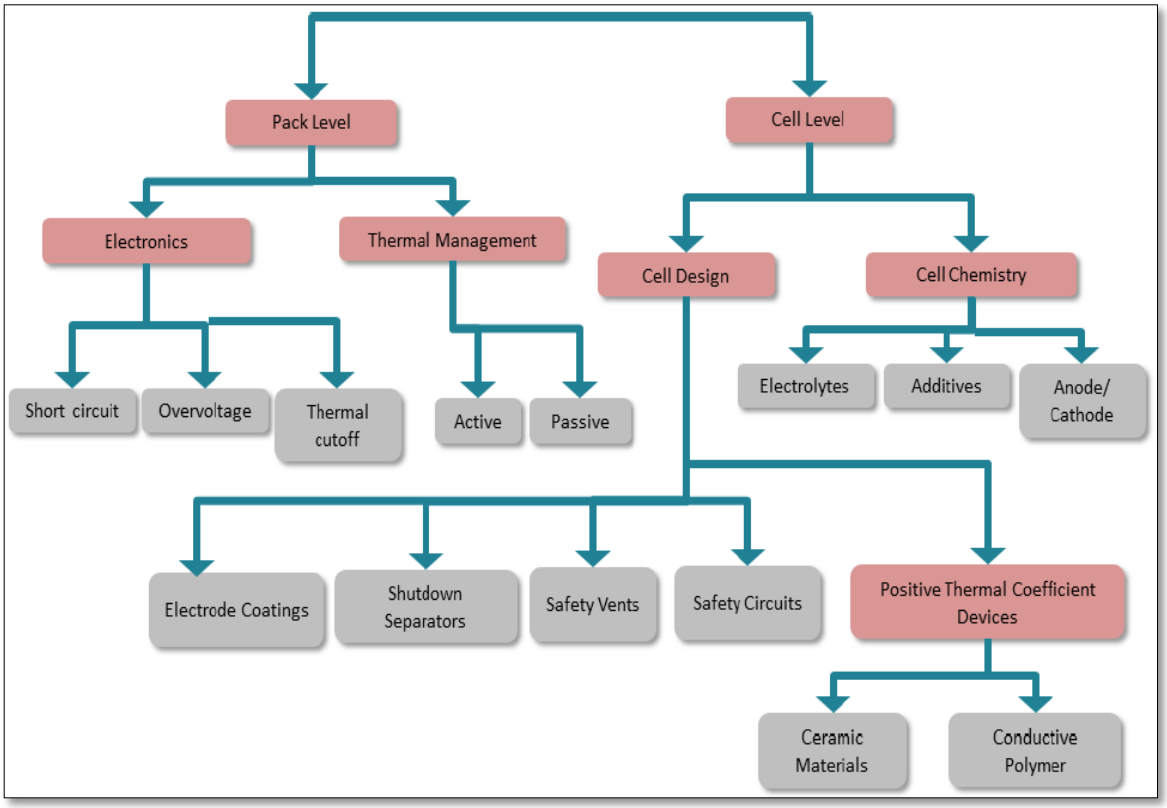


**Figure II.13:** *Lithium-ion Safety Mechanisms [57].*

f) **Voltage Comparaison**

The most important factor when determining whether lithium-ion and lead acid can be interchanged within a given electrical device is the voltage range of each chemistry.

The lithium-ion has good agreement with lead acid systems for a majority of the voltage range, but any electrical system would have to be able to accommodate the higher charging voltage of lithium-ion to get optimal performance [58]. Many battery charging controllers and discharge inverters with renewable energy are able to switch between lead acid and lithium-ion. Manufacturers of Charge Controllers and Inverters and lithium-ion companies may help to ensure compliance with the device.

g) **Additional Comparaison Table**

**Table II.4:** *Advantages and Limitations of Lead Acid Batteries [59,60].*

| Advantages and Limitations of Lead Acid Batteries | |
|---|---|
| Advantages | Inexpensive and simple to manufacture — in terms of cost per watt hours, the SLA is the least expensive.<br><br>Mature, reliable and well-understood technology — when used correctly, the SLA is durable and provides dependable service.<br><br>Low self-discharge — the self-discharge rate is among the lowest in rechargeable battery systems.<br><br>Low maintenance requirements — no memory; no electrolyte to fill. |
| Limitations | Cannot be stored in a discharged condition.<br><br>Low energy density — poor weight-to-energy density limits use to stationary and wheeled applications.<br><br>Allows only a limited number of full discharge cycles — well suited for standby applications that require only occasional deep discharges.<br><br>Environmentally unfriendly — the electrolyte and the lead content can cause environmental damage.<br><br>Transportation restrictions on flooded lead acid — there are environmental concerns regarding spillage in case of an accident. |

**Table II.5:** *Advantages and Limitations of Li-ion Batteries [59,60].*

| Advantages and Limitations of Li-ion Batteries | |
|---|---|
| Advantages | High energy density — potential for yet higher capacities.<br>Relatively low self-discharge — self-discharge is less than half that of NiCd and NIMIHE<br>Low Maintenance — no periodic discharge in needed; no memory. |
| Limitations | Requires protection circuit — protection circuit limits voltage and current. Battery is safe if not provoked.<br>Subject to aging, even if not in use — storing the battery in a cool place and at 40 percent state-of-charge reduces the aging effect.<br>Moderate discharge current.<br>Subject to transportation regulations — shipment of larger quantities of Li-ion batteries may be subject to regulatory control. This restriction does not apply to personal carry-on batteries.<br>Expensive to manufacture — about 40 percent higher in cost than NiCd. Better manufacturing techniques and replacement of rare metals with lower cost alternatives will likely reduce the price.<br>Not fully mature — changes in metal and chemical combinations affect battery test results, especially with some quick test methods. |

## II.6. Conclusion

In this chapter, we learned about how to charge batteries and their models. Where we discussed the different types of batteries, and we talked in depth about lithium batteries and lead acid batteries, because they are the most used and we noticed that they are the most efficient. But we will discuss in the next chapter the study of the lead acid battery, because it is available. We will also choose the generic battery model because it is the easiest in the principle of work.

# Chapter III:

# Coulomb Counting Method Estimation

## III.1. Introduction

This chapter proposes a method for estimating lead acid batteries by SOC based on coulomb counting.

For safe usage, the battery operating current and voltage are specified by manufacturers [63]. The proposed SOC system; however, depends only on the charges that have flowed into and out of the battery within the safe operating range. Obviously, the precision of the SOC estimation process is influenced by the efficiencies of discharge and charging under varying ambient temperature.

## III.2. Coulomb Counting Method

The Coulomb Counting method, also called the method of current integration, is based on calculating the number of ampere hours in and out of a battery, [Alzieu et. al, 1997]. The accuracy of this method depends mainly on the resolution of the current sensor. This counting should reflect the coulombic efficiency depending on the charge or discharge rate. However, these methods allow the determination of relative changes of charge's state only without taking into account the self-discharge [64].

The determination of the charge's state, therefore, requires knowledge of the initial state of charge [65, 66]. The charge's state of the battery estimation based on this method is as following [67]:

$$\boldsymbol{SOC = SOC_0 - \frac{100}{C_n} \int_{t_0}^{t} \eta . I(\tau) d} \qquad \textbf{(III.1)}$$

If the initial value of the state of charge $SOC_0$ is specified, the coulomb counting method becomes very precise and particularly easy to determine the SOC. But if the $SOC_0$ is not known, this method is less accurate.

In addition, the coulombic efficiency, which depends on the operating conditions (SOC, temperature, current and so on) [1, 38], is difficult to obtain. As the current sensor may introduce an offset that increases the imprecision of this estimation. With time, all these factors contribute to the increasing of the SOC error, especially in the reserve batteries (Back-up) and in packs for hybrid electric vehicle (HEV). However, the method of coulomb counting is widely used in practice because of its simplicity [67].

N. K. Soon et al [68] proposed an intelligent estimation approach based on the coulomb counting method from the characteristics of charge and discharge of Lithium-Ion batteries.

Their proposed method has proven its efficiency and accuracy, and this through several experiments conducted over lithium-ion batteries.

F. Feng et al [69] used a method of estimation of the SOC combining the improved method of Ampere-hour (Ah) counting and the method of Open Circuit Voltage (OCV). However, the improved method of Ah counting may affect the available capacity and the coulombic efficiency, and thus, depending on the temperature during the calculation of SOC. In addition, the SOCs of the battery with different temperatures can be mutually converted according to the loss of capacity. The method of open circuit voltage (OCV) is used to offset accumulation error in Ah counting caused by the low accuracy of current sensors and the lack of specific initial SOC for calibration and as a supplement as well.

## III.3. Generic Battery Model

### III.3.1. State of the Art

In [70], Olivier Tremblay and Louis-A. present an improved and easy-to-use battery dynamic model. The charge and the discharge dynamics of the battery model are validated experimentally with four batteries types. An interesting feature of this model is the simplicity to extract the dynamic model parameters from batteries datasheets. Only three points on the manufacturer's discharge curve in steady state are required to obtain the parameters. Finally, the battery model is included in the SimPowerSystems simulation software and used in a detailed simulation of an electric vehicle based on a hybrid fuel cell-battery power source. The results show that the model can accurately represent the dynamic behaviour of the battery.

S.M.Wijewardena in [71], presents mathematical modelling and dynamic simulation of battery storage systems can be challenging and demanding due to nonlinear nature. Simulation in time domain could be time consuming as battery storage (BS) systems do not behave according to readily available mathematical functions. Economic advantages, partial sustainability and the portability of these units pose promising substitutes for backup power systems in hybrid vehicles, hybrid electricity power generation systems, telecommunication exchanges and computer networks. Though, there have been many research papers published in this area with complex mathematical models and simulation systems, each system has its own constraints and specific applications. The aim of this research is to present a suitable convenient and dynamic battery model that can be used to model a general BS system. The proposed new dynamic battery model has the capability to analyse the effect of temperature, cyclic charging/discharging, and voltage stabilization effects. Simulink has been used to study

the characteristics of the system and the proposed system has produced very good successful results.

In [72], Essam M. Allam. Presents battery model applied to dynamic simulation software. Simulation using nickel hydrogen battery model thus makes it possible to analyses very complex phenomena. The model was realized in MATLAB / Simulink software packages. The battery block implements a generic dynamic model parameterized to represent most popular types of rechargeable batteries. In this case, the battery's model parameters are not exactly the same as those of the electric vehicle battery but it is nevertheless possible to study, with good precision, phenomena caused by the battery. Moreover, this model helps to develop the energy management system (EMS) which controls the flow of energy between the solar panels and battery. Finally, it is possible to control the charge and the discharge of the battery with precision. The results obtained show that the use of this battery model makes it possible to properly represent the transient states. It is thus possible to analyses them in order to fine-tune the various control devices and they show accurately the general behavior of the battery. The battery monitoring system developed is used to prevent people from being stranded. This device makes sure that no matter what, a car will be able to start and that a person will not be left with a dead battery.

### III.3.2. **Charge / Discharge of this Model in MATLAB Simulink 2013**

The battery block implements the parameterized dynamic model which represents different types of rechargeable batteries:

- Lead Acid Model
- Lithium-ion Model
- Nickel-Cadium Model
- Nickel-Metal-Hybrid Model

The general charge and discharge model is:

Fig. III.3 shows the equivalent electrical circuit of the battery in MATLAB Simulink.

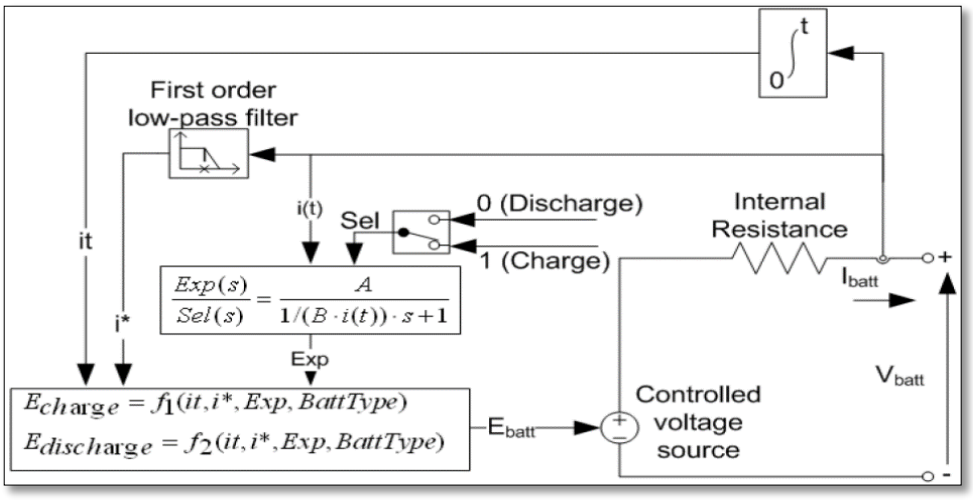


**Figure III.1:** *Battery Charge / Discharge Pattern.*

In this research, we studied the lead acid model because it is the available in our country, Algeria.

The general charge and discharge model are:

- ✓ ***Discharge Model (i*>0)***

$$f_1(it, i*, i, Exp) = E_0 - K.\frac{Q}{Q-it}.i* - K.\frac{Q}{Q-it}.it + Laplace^{-1}\left(\frac{Exp(s)}{Sel(s)}.0\right)$$

- ✓ ***Charge Model (i*<0)***

$$f_2(it, i*, i, Exp) = E_0 - K.\frac{Q}{it+0.1.Q}.i* - K.\frac{Q}{Q-it}.it + Laplace^{-1}\left(\frac{Exp(s)}{Sel(s)}.\frac{1}{s}\right)$$

This model is based on assumptions and limitations.

**A. The Assumptions**

- The parameters of the model are deduced from the characteristics of the discharge and assumed the same for the charge.
- The capacity of the battery does not change with the amplitude of the current.
- No effect of temperature in the behavior of the model.
- Self-discharge of the battery is not shown.

**B. The Limitations**

- The minimum voltage of the battery without load is 0 V and the maximum of this is 2 * $E_0$.
- The minimum capacity of the battery is 0 Ah and the maximum capacity is Q.

## III.4. Application

The parameters in tables 1,2 and 3 are extracted from the data sheet.

**Table III.1:** *Parameters of our Battery at 0.25C.*

| | |
|---|---|
| **Nominal Voltage (V)** | 12 |
| **Rated Capacity (Ah)** | 52 |
| **Initial State of Charge (%)** | 100 |
| **Maximum Capacity (Ah)** | 40.1999 |
| **Fully Charged Voltage (V)** | 12.7 |
| **Nominal Discharge Current (A)** | 13 |
| **Internal Resistance (ohms)** | 0.0055 |
| **Capacity (Ah) @ Nominal Voltage** | 38.2 |
| **Exponential Zone [Voltage(V), Capacity (Ah)]** | [12.7 2.5] |

**Table III.2:** *Parameters of our Battery at 0.17C*

| | |
|---|---|
| **Nominal Voltage (V)** | 12 |
| **Rated Capacity (Ah)** | 52 |
| **Initial State of Charge (%)** | 100 |
| **Maximum Capacity (Ah)** | 53.8 |
| **Fully Charged Voltage (V)** | 12.8 |
| **Nominal Discharge Current (A)** | 13 |
| **Internal Resistance (ohms)** | 0.0055 |
| **Capacity (Ah) @ Nominal Voltage** | 44.80 |
| **Exponential Zone [Voltage(V), Capacity (Ah)]** | [12.8 1.9] |

**Table III.3:** *Parameters of our Battery at 0.09C*

| | |
|---|---|
| **Nominal Voltage (V)** | 12 |
| **Rated Capacity (Ah)** | 52 |
| **Initial State of Charge (%)** | 100 |
| **Maximum Capacity (Ah)** | 47.5 |
| **Fully Charged Voltage (V)** | 12.9 |
| **Nominal Discharge Current (A)** | 13 |
| **Internal Resistance (ohms)** | 0.0055 |
| **Capacity (Ah) @ Nominal Voltage** | 46 |
| **Exponential Zone [Voltage(V), Capacity (Ah)]** | [12.9 2.225] |

## III.5. Simulation Results and Discussions

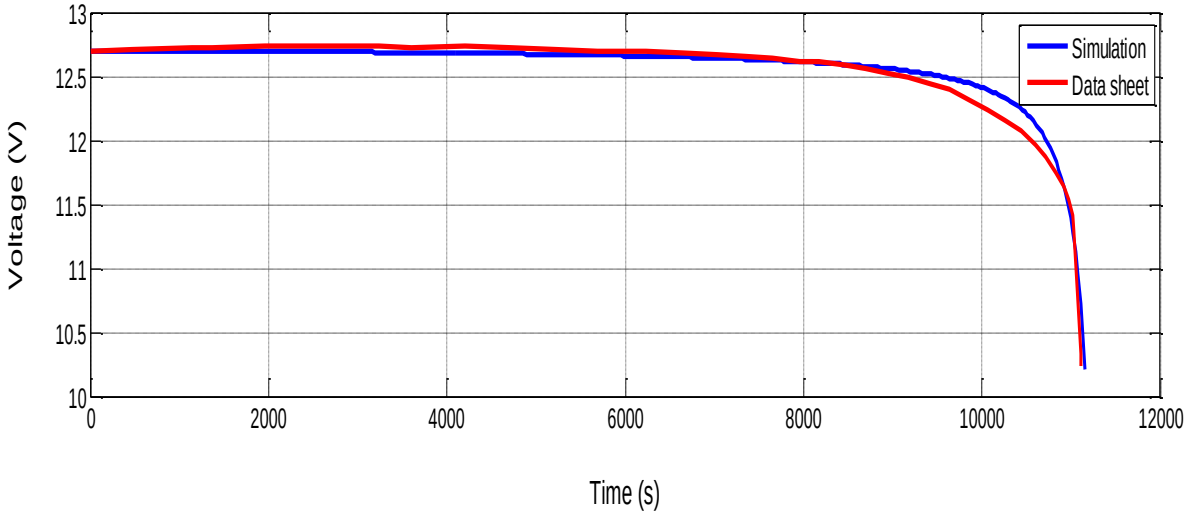


**Figure III.2:** *Discharging Voltage as a Function of Time at '0.25C'.*

The figure. III.2 above shows that the discharge voltage of the datasheet battery and the simulation are slightly different and although it differs due to the precision when extracting the parameters from the battery model (Table. III.1) from the discharge voltage curve given by the manufacturer. The discharge voltage decreases for 3.05 hours up to 10.2V, this value calls the cut-off voltage, i.e. when the battery discharge voltage reaches this value, it disconnects the

battery. The value of 10.2 V is suitable for the value of the minimum SOC is equal to 20%. That is to say that the voltage given by the manufacturer is noted with ideal conditions (T = 25C°, Idisch = 13A). The two curves (datasheet and simulation) are pasted.

This shows that the model of the battery used is to present the real behavior of the battery in the discharge phase with good accuracy.

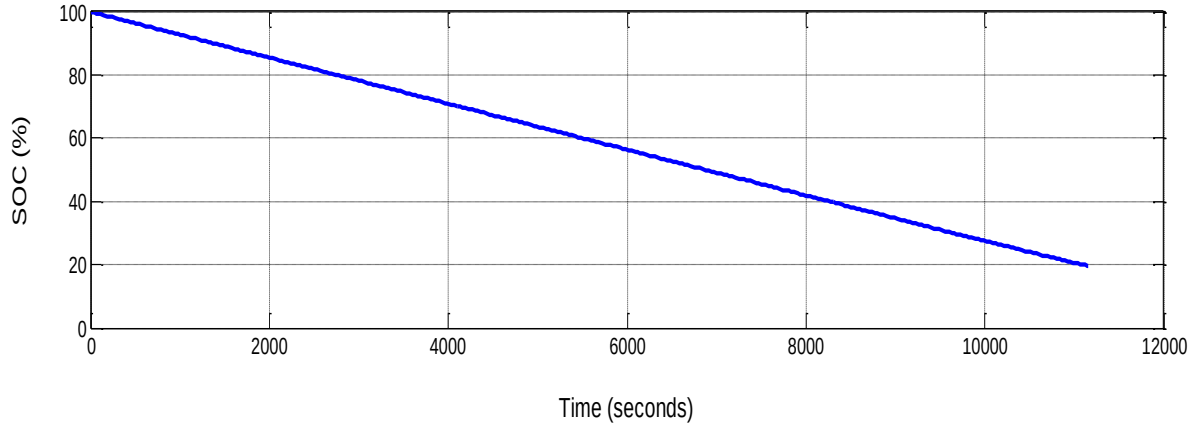


**Figure III.3:** *State-of-Charge as a Function of Time at '0.25C'.*

From the figure III.3 we note that the battery is initially fully charged (SOC(0) = 100%) and after 3.05 h the state of charge of the battery decreases to the minimum value (SOC = 20%) this value corresponds to the actual value of the lead-acid battery.

The SOC curve estimated by the coulomb counting estimator is a straight line, i.e. the battery is discharged under a constant discharge current (Idisch = 13A), this technique tracks the state of charge of the battery during the entire discharge time (3.05 hours).

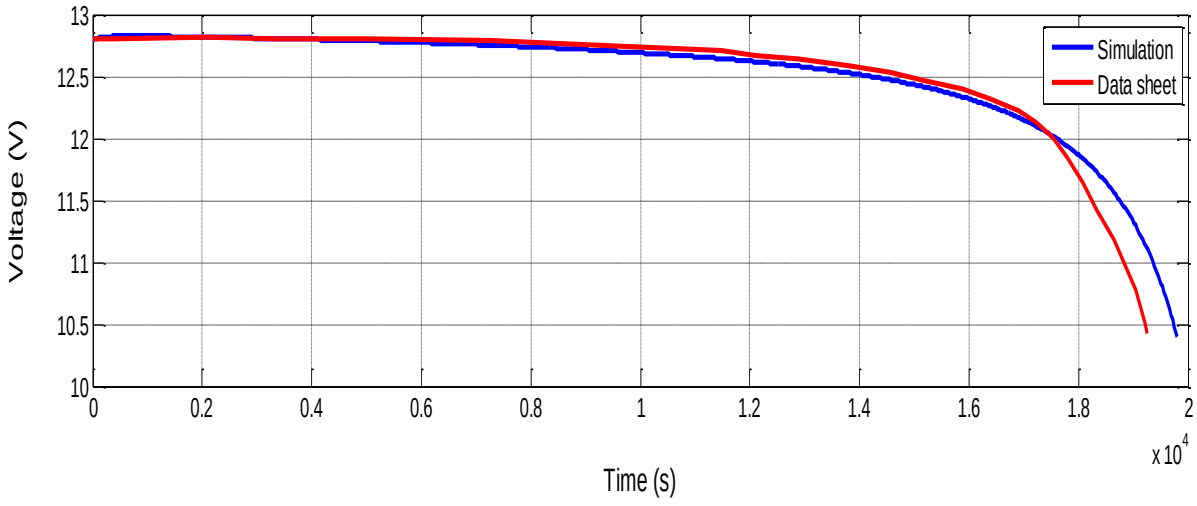


**Figure III.4:** *Discharging Voltage as a Function of Time at '0.17C'.*

The figure. III.4 shows that the discharge voltage of the datasheet battery and the simulation are slightly different and although it differs due to the precision when extracting the parameters from the battery model (Table. III.2) from the discharge voltage curve given by the manufacturer. The discharge voltage decreases for 5.27 hours up to 10.4V, this value calls the cut-off voltage, i.e. when the battery discharge voltage reaches this value, it disconnects the battery.

The value of 10.4 V is suitable for the value of the minimum SOC is equal to 20%. That's to say that the voltage given by the manufacturer is noted with ideal conditions: (T = 25C°, Idisch = 8.84A). The two curves (datasheet and simulation) are pasted. This shows that the model of the battery used is to present the real behavior of the battery in the discharge phase with good accuracy.

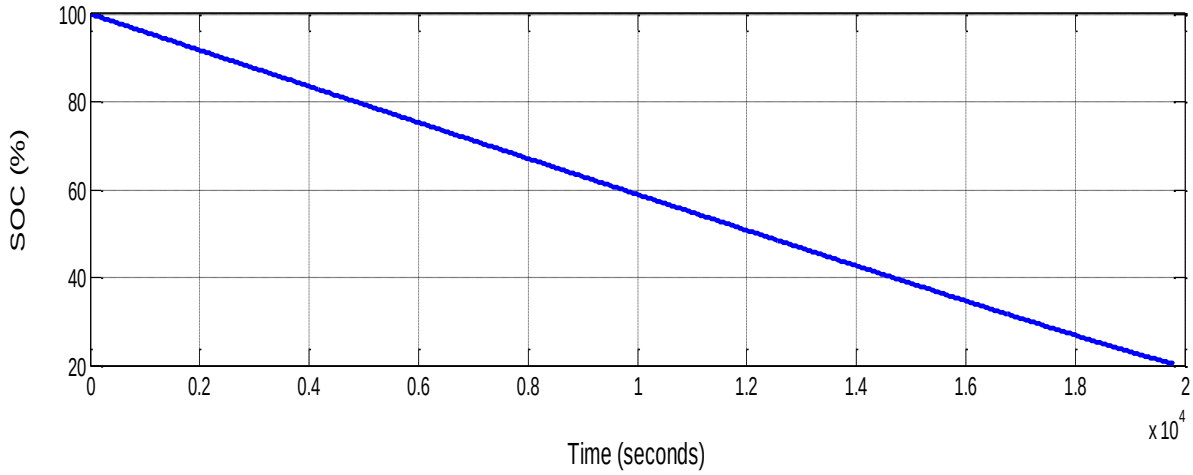


**Figure III.5:** *State-of-Charge as a Function of Time at '0.17C'.*

In the figure III.5 above, we note that the battery is initially fully charged (SOC(0)=100%) and after 5.27 h the state of charge of the battery decreases to the minimum value (SOC = 20%) this value corresponds to the actual value of the lead-acid battery.

The SOC curve estimated by the coulomb counting estimator is a straight line, i.e. the battery is discharged under a constant discharge current (Idisch = 8.84 A), this technique tracks the state of charge of the battery during the entire discharge time (5.27 hours).

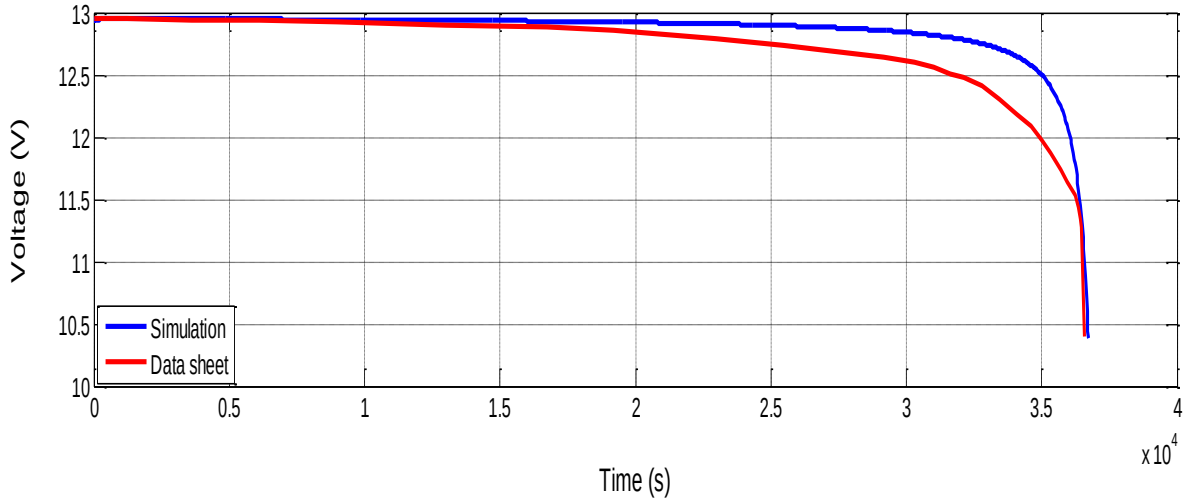


**Figure III.6:** *Discharging Voltage as a Function of Time at '0,09C'.*

The figure. III.6 above shows that the discharge voltage of the datasheet battery and the simulation are slightly different and although it differs due to the precision when extracting the parameters from the battery model (table. III.3) from the discharge voltage curve given by the manufacturer.

The discharge voltage decreases for 10.20 hours up to 10.5V, this value calls the cut-off voltage, i.e. when the battery discharge voltage reaches this value, it disconnects the battery. The value of 10.5 V is suitable for the value of the minimum SOC is equal to 20%. That is to say, the voltage given by the manufacturer is noted with ideal conditions (T = 25C °, Idisch=4.68 A) .

The two curves (datasheet and simulation) are pasted. This shows that the model of the battery used is to present the real behavior of the battery in the discharge phase with good accuracy.

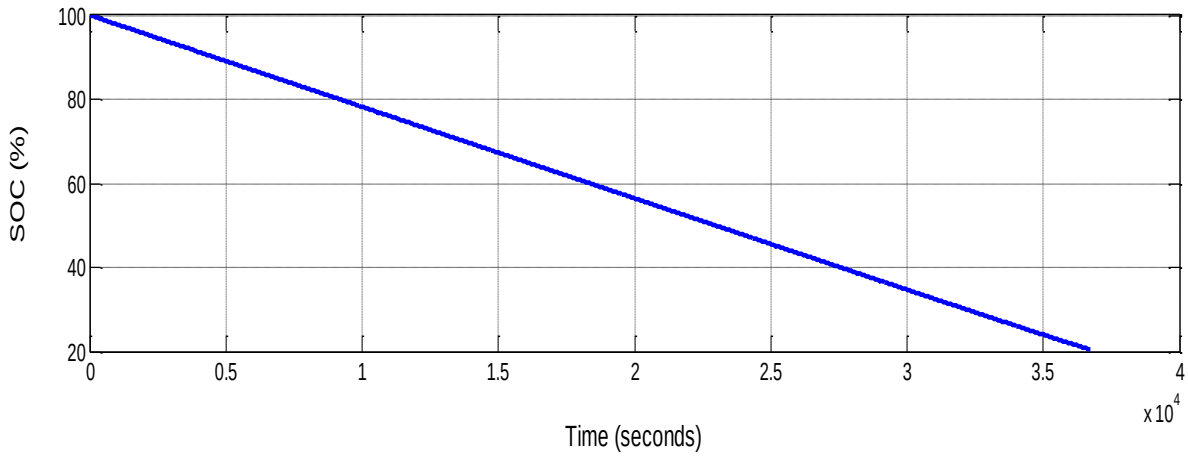


**Figure III.7:** *State-of-Charge as a Function of Time at '0.09C'.*

In the figure III.7 above, we note that the battery is initially fully charged (SOC(0)=100%) and after 10.20 hours (in order) the state of charge of the battery decreases to the minimum value (SOC = 20%) this value corresponds to the actual value of the lead-acid battery.

The SOC curve estimated by the coulomb counting estimator is a straight line, i.e. the battery is discharged under a constant discharge current (Idisch = 4.68A), this technique tracks the state of charge of the battery during the entire discharge time (10.20 hours).

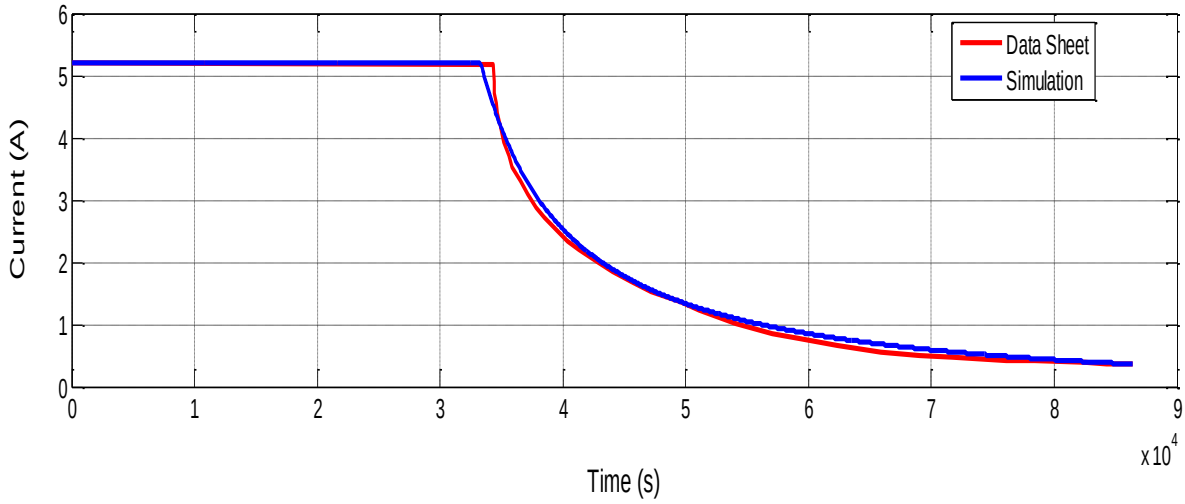


**Figure III.8:** *Current Voltage as a Function of Time.*

Fig. III.8 illustrates that the initial value of the battery charge current in the two curves (datasheets and simulation) its value equal to 5.5A.

We notice that the charge current remains constant for 3.50h at a value of 5.5A in (datasheets and simulation) then the value begins to decrease until reaching a value of 0.29A in all the curves, that is to say we distinguish two areas on the curve where the first is from [0 to 3.50] h in the simulation and datasheet curves, intended for the charging mode by a constant current (CC) and the second from [3.50 to 24] h intended for the mode of charge by a constant voltage (CV) [73].

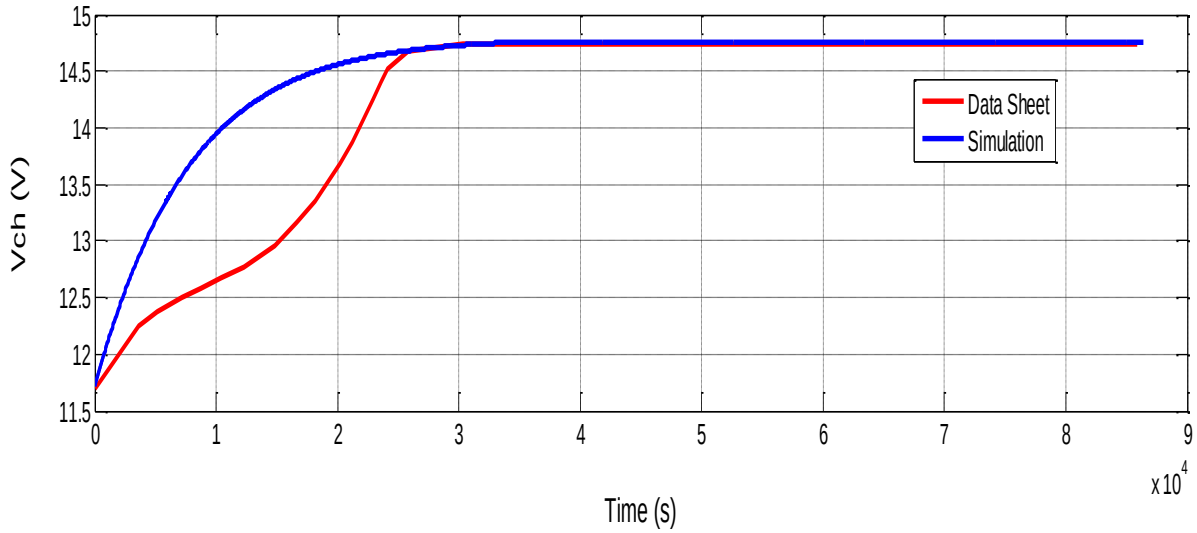


**Figure III.9:** *Charging Voltage as a Function of Time.*

Figure III.9 illustrates that the initial value of the battery charge voltage in the two curves (simulation and datasheets) has a value equal to 11.6V.

We note that the charging voltage increases rapidly to 14.7 V and stabilizes in this value, that is to say, there are two zones on the curve where the first is from [0 to 3] destine for the charging mode by constant current (CC) and the second from [3 to 24] h destine for the charging mode by a constant voltage (CV) , the only difference between the two curves (simulation and datasheet) is in the charging zone by a constant current because the parameters of the simulation in the discharge phase are the same for the charge phase because in reality the charge phase depends on several factors (charging mode, SOC(0), ambient temperature and so on).

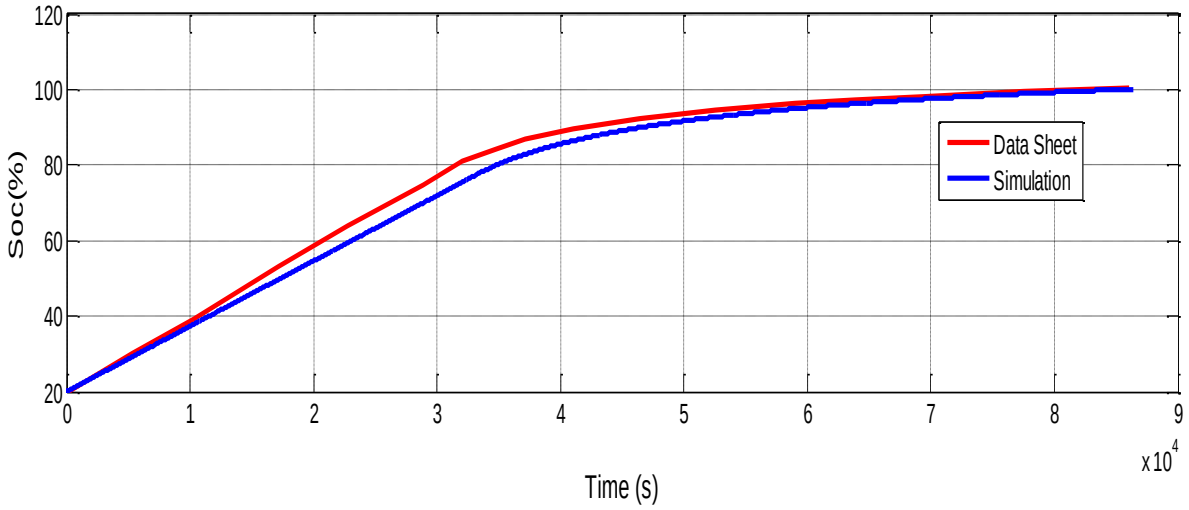


**Figure III.10:** *The State of Charge as a Function of Time 'Charge Test'.*

According to Figure. III.10, we note that SOC (0) = 20% at time t = 0 and increases with the charging time up to 100%, i.e. the battery is fully charged. There are two parts in the curve, the first part is between [0 3] h, wich corresponds to the constant current charging mode, it is linear. This part is characterized by the rapid variation of SOC as a function of time for example at 3h SOC (datasheet) = 80% and SOC (simulation) = 70%. The second part is in the form of a bending line. It corresponds to the charging mode at constant voltage. This part is characterized by the slow variation of the SOC for example from [3 24] h the SOC (datasheet) increases by 20% and the SOC (simulation) increases by 30%. So, we can say that the battery charging capacity is dependent on the charging mode, it is faster in CC mode and slower in CV mode, that is why the newer charger is faster to gain more of time especially the case of lead-acid batteries.

## III.6. Conclusions

The charging and discharging characteristics of lead acid batteries were studied carefully. To improve the estimation accuracy, the correction of the operating efficiency and the evaluation of the SOC were both considered. Through the investigation, the following noteworthy conclusions are obtained:

- The battery can be regarded as completely exhausted when its voltage drops to the cut-off voltage, so that SOC can be reset to zero at this point.
- The model of the battery used in SimPowerSystem (MATLAB Simulink) is less precise in charging mode and very precise in discharging mode and presents the behavior of the battery in the constant current discharge phase.
- The estimator of the state of charge of the battery by the coulomb counting method is very precise.

# Chapter IV:

# Experimental Results and Discussion

## IV.1. Introduction

In this chapter, we study the coulomb counting method to estimate the state of charge of the battery (SOC), without taking into account the effect of temperature and the Peukert effect.

The objective of this chapter is to make a comparison of the theoretical and practical SOC to justify the battery model and to show the efficiency of our method.

## IV.2. Experimentation and Validation of Results

### IV.2.1. Description of The Test Bench

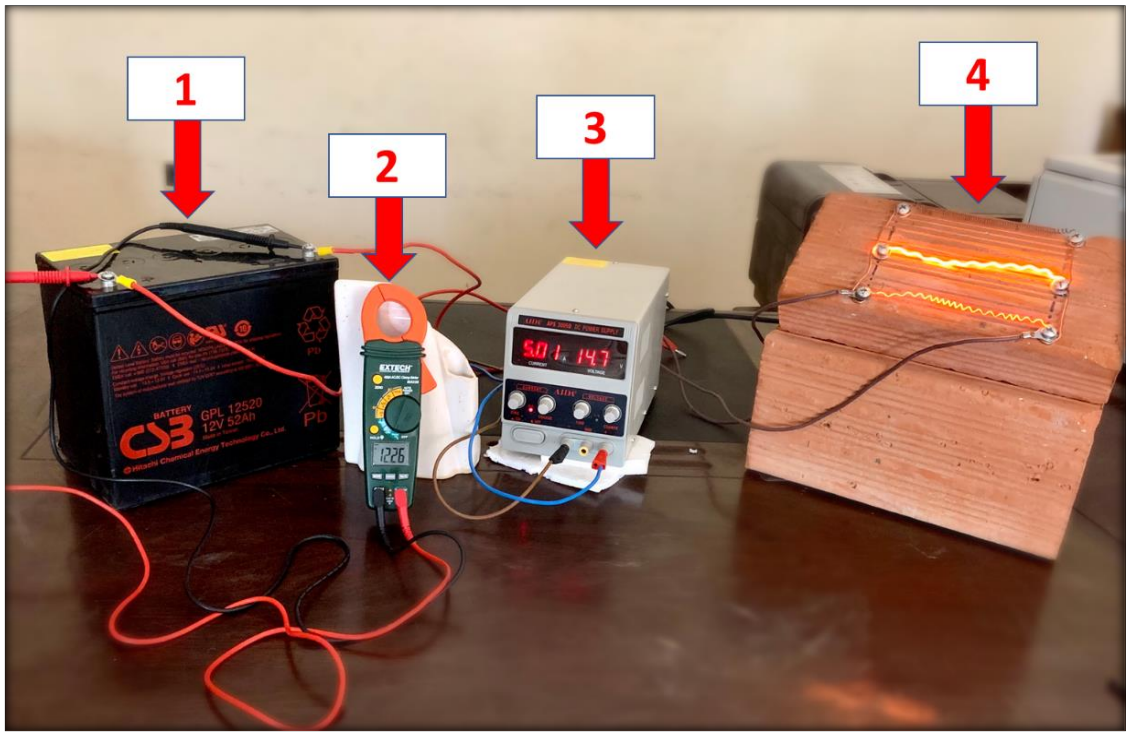


**Figure IV.1:** *Test Bench*

1.A Lead Acid Battery

2.Clamp Meter

3.DC Power Supply

4.A Variable Resistor (Handmade)

### IV.2.2. **Test Procedure**

#### **Charge Test**

We charge the battery with a stabilized power supply, before connecting the battery we set the charging voltage to 14.7V. We limit the current to a maximum of 5.03A (this is the maximum value that we have). We plug in the battery and we leave it until it is fully loaded and of course with the clamp meter and the hall effect sensor we read the voltage and the charging current of the battery every 10 minutes. The end-of-charge voltage equal Vfinish-ocv=13.96V and the end-of-charge current, when the minimum value of the current that can reach in this test is Imin = 0.29A. When the charging current reaches the minimum value, which gives by the manufacturer 0.29A by disconnecting the battery and we cut the voltage of the stabilized power supply.

This test was carried out for 02 days, the duration of this test equal to Tch = 1440min or Tch = 24h

#### **Discharge Test**

We have 3 experiments in this test:

- The first experiment: a variable resistor is connected (to adjust it to a discharge current equal to 13A) with the battery, and the voltage and the discharge current are read every 5 minutes, by the measuring of clamp meter for 3.05 hours. After 3.05 hours, it reaches the end of discharge voltage (cut-off voltage) equal to 10.10V in this case, disconnecting the discharge resistance. The discharge resistance equal to Rdisch = 0.96-1Ω and the ambient temperature T = 26.7 ° C.
- The second experiment: the variable resistor is connected (to adjust it to a discharge current equal to 8.84A) with the battery, and the voltage and the discharge current are read every 5 minutes, by the of clamp meter for 5.41 hours. After 5.41 hours it reaches the end of discharge voltage (cut-off voltage) equal to 10.37V in this case disconnecting the discharge resistor. The discharge resistance equal to Rdisch = 1.42-1.50Ω and the ambient temperature T = 28.6 ° C.
- The third experiment: the variable resistor is connected (to adjust it to a discharge current equal to 4.68A) with the battery, and the voltage and the discharge current are read every 5 minutes, by the measuring of clamp meter for 10.25 hours. After 10.25 hours it reaches the end of discharge voltage (cut-off voltage) equal to 10.39V; in this

case, disconnecting the discharge resistor. The discharge resistance equal to Rdisch = 2.69-3Ω and the ambient temperature T = 26.1 ° C.

## IV.3. Results and Discussions

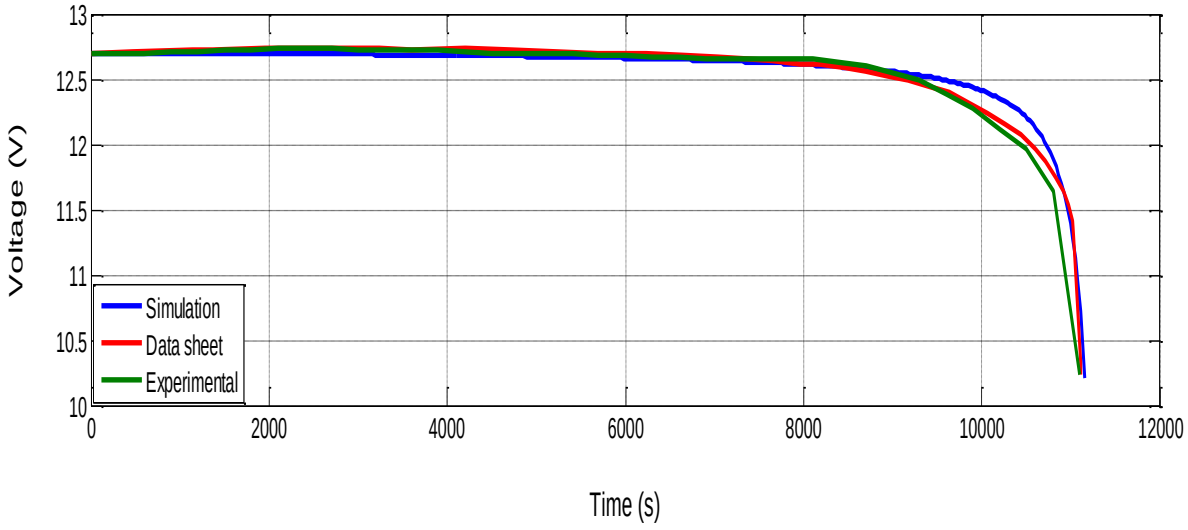


**Figure IV.2:** *The Discharge Voltage as a Function of Time at 0.25C*

The discharge voltage decreases for 3.05 hours to 10.10V, this value calls the cut-off voltage, i.e. when the battery discharge voltage has reached this value, we disconnect the battery in order not to damage it.

The value of 10.10 V does not correspond to the complete discharge of the battery (SOC = 0%) but it is suitable for the value of the minimum SOC which is equal to / close to 20% [74].

The experimental discharge voltage is stuck on that of the simulation except that the value of the end-of-charge voltage (10.10 V) is reached before a duration of T = 3h 30 min, this difference shows that the battery capacity is varied according to the parameters of use (charging mode, ambient temperature, discharge current, and so on). That is to say, the voltage given by the manufacturer is recorded with ideal conditions (T = 25C °, Idisch = 13A, the state of aging of the battery (SOH = 0%) that is say a new battery).

The three curves (datasheet, simulation and experimental) are almost glued, this shows that the model of the battery used presents the real behavior of the battery in the discharge phase with very high precision.

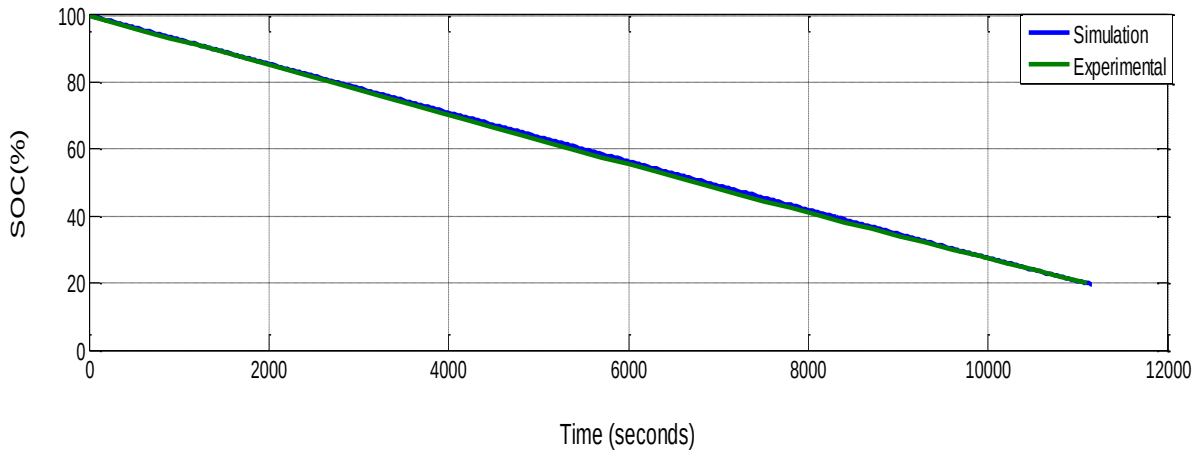


**Figure IV.3:** *The State of Charge of the Battery (SOC) as a Function of Time at 0.25C*

According to figure IV.3 above, we notice that the battery is initially full charged (SOC(0) = 100%) and after 3.05 hours the state of charge of the battery decreases to the minimum value (SOC = 20%) this value corresponds to the real value of the lead-acid battery (SOC min = 20%) [75], i.e. this value must not be exceeded in order not to damage the battery. The SOC curve estimated by the coulomb counting estimator is a straight line, i.e. the discharge of the battery is done under a constant discharge current (Idisch = 13A), this technique follows the state of charge of the battery during the entire discharge period (3.05 hours).

SOC experimental and SOC simulation are glued. This shows that this technique is very precise and very robust, that is why it is very practical to use because of its simplicity and that it only requires a current sensor and a voltage sensor.

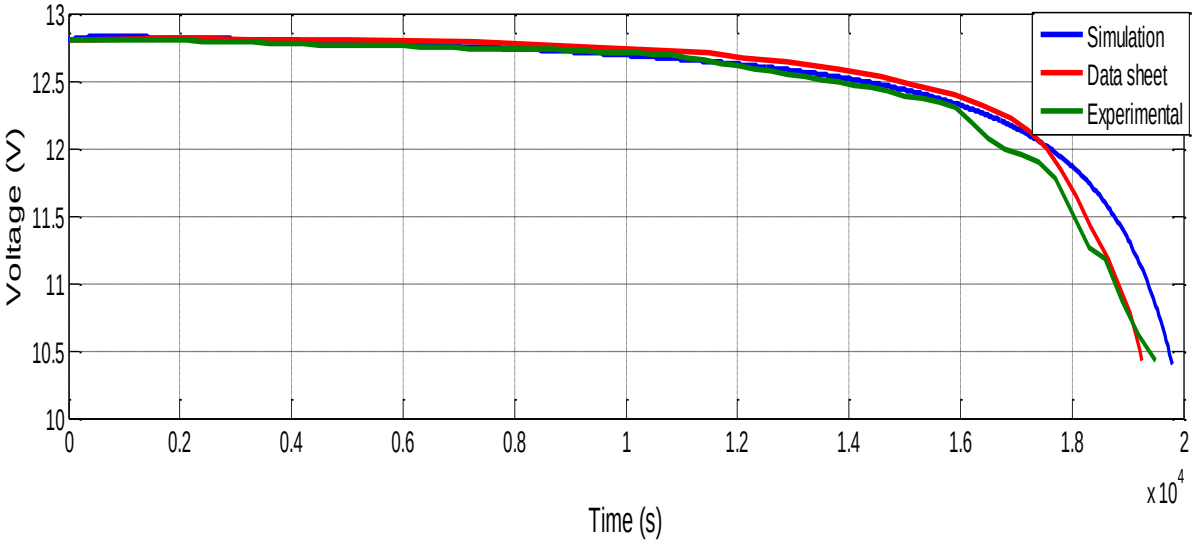


**Figure IV.4:** *The Discharge Voltage as a Function of Time at 0.17C*

The discharge voltage decreases for 5.41 hours to 10.37V, this value calls the cut-off voltage, i.e. when the battery discharge voltage has reached this value, we disconnect the battery in order not to damage it.

The value of 10.37 V does not correspond to the complete discharge of the battery (SOC = 0%) but it is suitable for the value of the minimum SOC is equal to close to 20% [74].

The experimental discharge voltage is stuck on that of the simulation except that the value of the end-of-charge voltage (10.37 V) is reached before a duration of T = 5h 24 min, this difference shows that the battery capacity is vary according to the parameters of use (charging mode, ambient temperature, discharge current, and so on). That is to say that the voltage given by the manufacturer is recorded with ideal conditions (T = 25C °, Idisch = 8.84A, the state of aging of the battery (SOH = 0%) that is say a new battery).

The three curves (datasheet, simulation and experimental) are almost glued, this shows that the model of the battery used presents the real behavior of the battery in the discharge phase with very high precision.

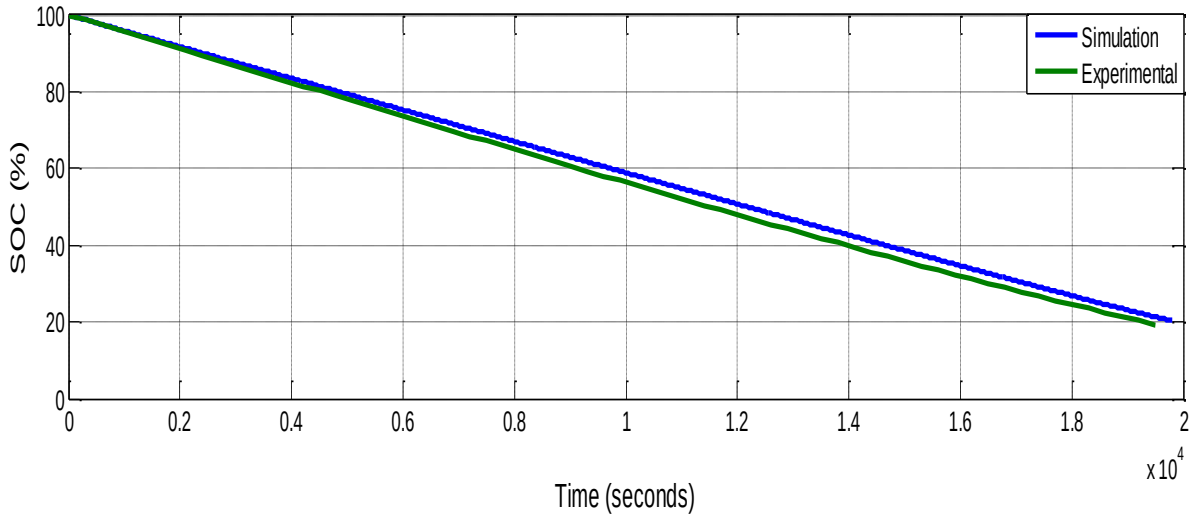


**Figure IV.5:** *The State of Charge of the Battery (SOC) as a Function of Time at 0.17C*

According to figure IV.5 Note that the battery is initially full charged (SOC(0) = 100%) and after 5.41 hours the state of charge of the battery decreases to the minimum value (SOC = 20%) this value corresponds to the real value of the lead-acid battery (SOC min = 20%) [75], i.e. this value must not be exceeded in order not to damage the battery.

The SOC curve estimated by the coulomb counting estimator is a straight line that is to say the discharge of the battery is done under a constant discharge current (Idisch = 8.84A), this

technique followed well the state of charge the battery during the entire discharge period (5.41h).

SOCexperimental and SOCsimulation are almost glued this shows that this technique is very precise and very robust, that is why it is very useful practically because of the simplicity and only requires a current sensor and a voltage sensor.

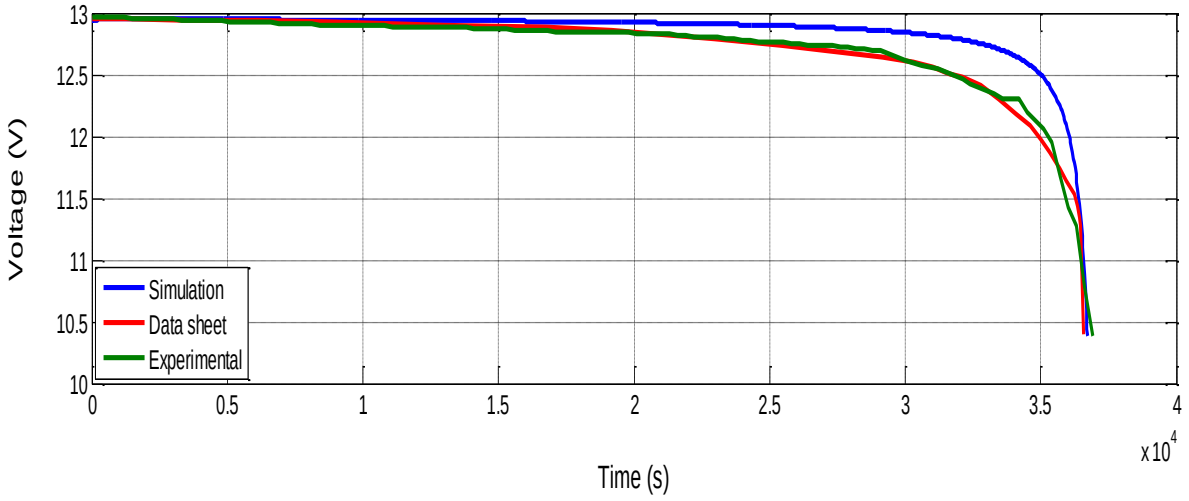


**Figure IV.6:** *The Discharge Voltage as a Function of Time at 0.09C*

The discharge voltage decreases for 10.25 hours to 10.39V, this value calls the cut-off voltage, i.e. when the battery discharge voltage has reached this value, we disconnect the battery in order not to damage it.

The value of 10.39 V does not correspond to the complete discharge of the battery (SOC = 0%) but it is suitable for the value of the minimum SOC is equal to close to 20% [74].

The experimental discharge voltage is stuck on that of the simulation except that the value of the end-of-charge voltage (10.39 V) is reached before a duration of T = 3h 30 min, this difference shows that the battery capacity is vary according to the parameters of use (charging mode, ambient temperature, discharge current, and so on). That is to say that the voltage given by the manufacturer is recorded with ideal conditions (T = 25C °, Idisch = 4.68A, the state of aging of the battery (SOH = 0%) that is say a new battery).

The three curves (datasheet, simulation and experimental) are almost glued, this shows that the model of the battery used presents the real behavior of the battery in the discharge phase with very high precision.

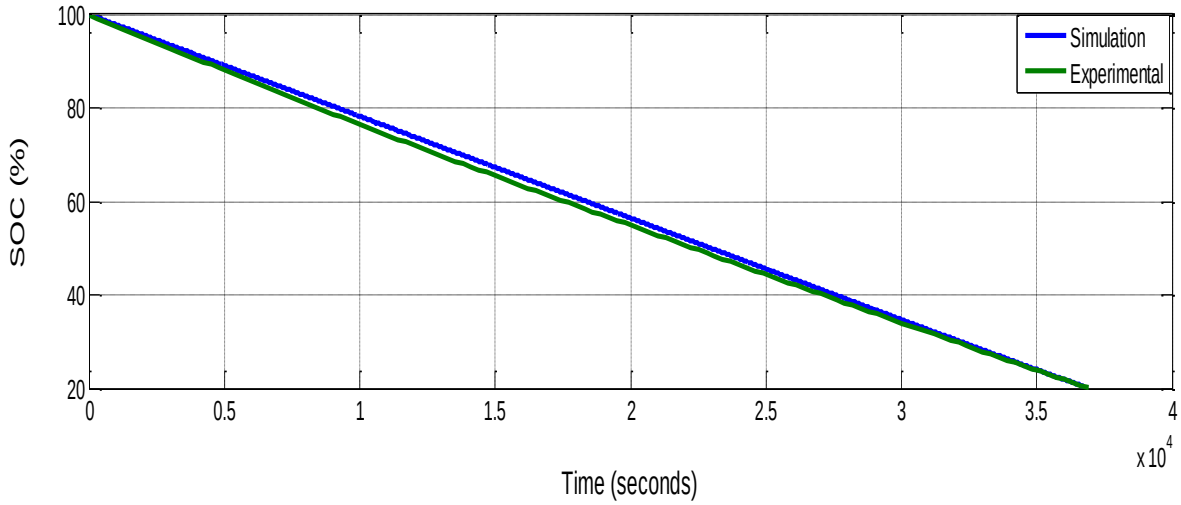


**Figure IV.7:** *The State of Charge of The Battery (SOC) as a Function of Time at 0.09C*

According to figure IV.7 Note that the battery is initially full charged (SOC(0) = 100%) and after 10.25 hours the state of charge of the battery decreases to the minimum value (SOC = 20%) this value corresponds to the real value of the lead-acid battery (SOCmin = 20%) [75], i.e. this value must not be exceeded in order not to damage the battery. The SOC curve estimated by the coulomb counting estimator is a straight line that is to say the discharge of the battery is done under a constant discharge current (Idéch = 4.68A), this technique followed well the state of charge of the battery during the entire discharge period (10.25h).

SOC experimental and SOC simulation are glued. This shows that this technique is very precise and very robust, that is why it is very useful practically because of the simplicity and only requires a current sensor and a voltage sensor.

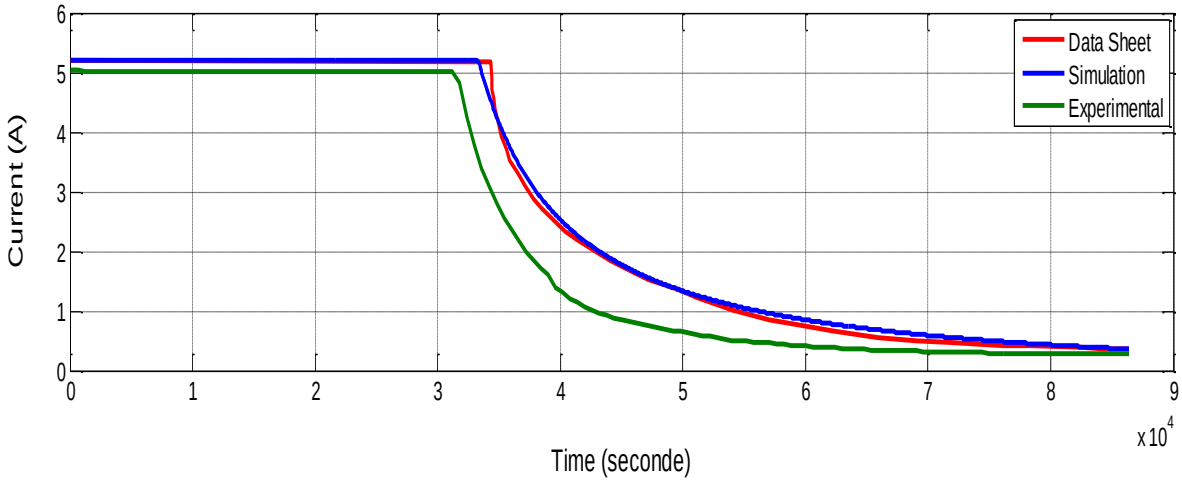


**Figure IV.8:** *The Charge Current as a Function of Time*

Fig. IV.8 illustrates that the initial value of the battery charge current in the two curves (datasheets and simulation) its value is equal to 5.5A and 5.03A in the experimental curve.

We notice that the charge current It remains constant for 3.50h at a value of 5.5A in (datasheets and simulation) and 5.03A in the experimental curve; then the value begins to decrease until reaching a value of 0.29A in all the curves. That is to say, we distinguish two areas on the curve where the first is [0 to 3.20] h in the curve of the experimental and from [0 to 3.50] h in the simulation and datasheet curves, intended for the charging mode by a constant current (CC) and the second from [3.20-3.50 to 24] h intended for the mode of charge by a constant voltage (CV) [75, 76], the only difference between the three curves (datasheet, simulation and experimental) is in the zone of charge by a constant current exactly in the initial value that we gave as a current for the battery, where in the experimental test we gave a value of 5.03A only, although the value of datasheet and simulation is 5.5A because that value represents the maximum value that our charger (DC POWER SUPPLY) can provide as a value of current.

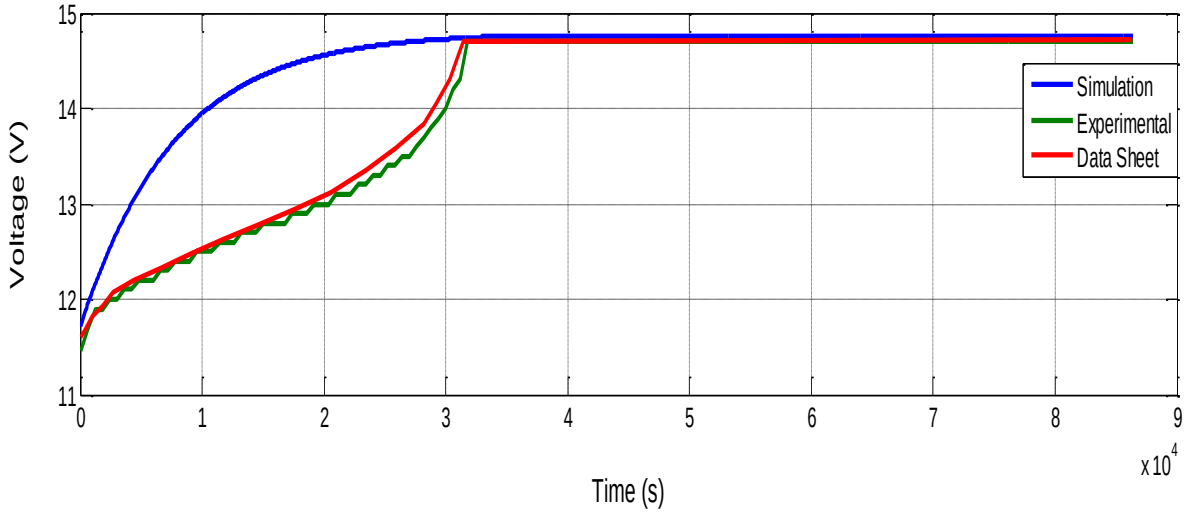


**Figure IV.9:** *The Charge Voltage as a Function of Time*

Fig. IV.9 illustrates that the initial value of the battery charge voltage in the three curves (experimental, datasheets and simulation) is equal to 11.6V; the latter is reflected by the initial state of charge or the quantity charge return to the battery, (takes SOC(0) = 20%) [74].

We notice that the charge voltage increases rapidly up to 14.7V and stabilizes in this value, that is to say we distinguish two areas on the curve where the first is [0 to 3] h in the curve of the experimental, datasheet and from [0 to 2.5] h in the simulation curve, intended for the charging mode by a constant current (CC) [75, 76] and the second from [3 to 20] h intended

for the mode of charge by a constant voltage (CV) [75, 76], the only difference between the three curves (experimental, datasheet and simulation) is in the zone of charge by a constant current (the duration of this phase is differed as in the curve datasheet and experimental is 3h and in the simulation curve is 2.5h, the nature of the curve) because the simulation parameters in the discharge phase are the same for the charge phase because that in reality, the charging phase depends on several factors (charging mode, SOC(0), ambient temperature, charging current and the charging voltage).

To avoid overcharging the battery by cutting our DC power supply, when the end-of-charge current is equal to 0.29A, this corresponds to a charge period equal to 24 hours.

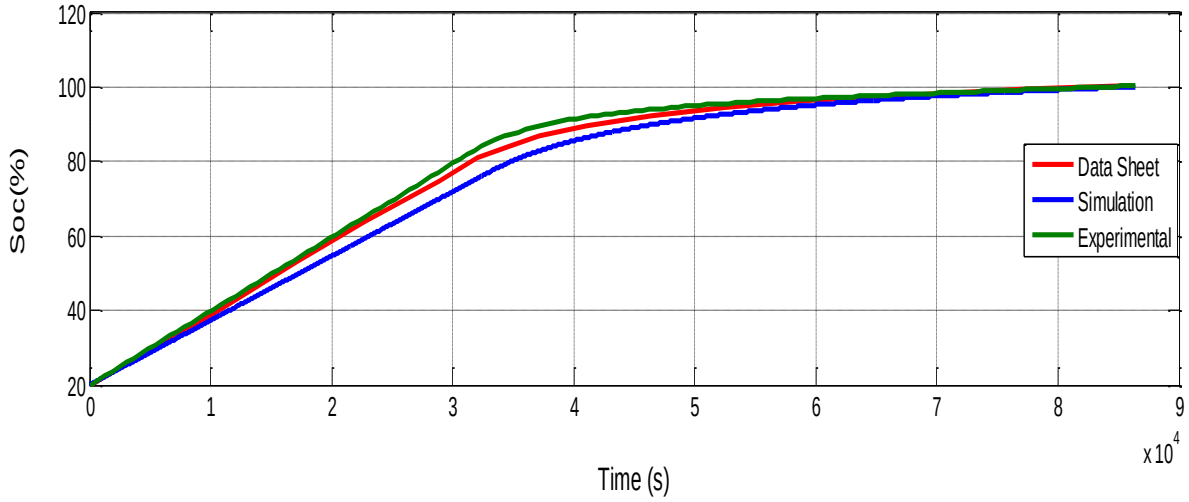


**Figure IV.10:** *The State of Charge of the Battery (SOC) as a Function of Time*

In Figure. IV.10, notice that SOC(0) = 0% (20%) at time t = 0 and increases with charging time up to 100% i.e. the battery is fully charged.

There are two parts in the curve, the first part is between [0 3.5] h, which corresponds to the constant current charging mode. It is linear in form. This part is characterized by the rapid variation of the SOC as a function of time for example at 3.5h SOC (experimental) = 85%, SOC (datasheet) = 83% and SOC (simulation) = 80% the second part is in the form of a curve line. It corresponds to the charging mode at constant voltage, it is characterized by the slow variation of the SOC. For example, [3.5 24] h the SOC (experimental) increases by 15%, SOC (datasheet) increases by 17% and the SOC (simulation) increases by 20%.

So, we can say that the battery charge capacity is dependent on the charging mode, it is faster in CC mode and slower in CV mode, that's why the new charger is faster to gain more time especially in the lead-acid batteries.

From this figure it can be seen that the coulomb counting method followed well the SOC during the entire charge, so we can say that this method does not depend on the model and technology of the battery.

## IV.4. Conclusion

Based on the obtained results, we can conclude that:

- The battery model used in MATLAB Simulink is less precise in charge mode and very precise and presents the behavior of the battery in the constant current discharge phase.
- The estimator of the state of charge of the battery by the coulomb counting method is very precise and no longer used in practice.
- The disadvantage of this technique is the imprecision and the difficulty of finding the initial SOC.

# General Conclusion

# General Conclusion

The main objective of this thesis was to establish a battery charge estimator based on a series of charge / discharge tests in order to develop an accurate estimator.

This estimate will depend on the battery technology, its electrical characteristics but also the ambient temperature. So, this information on the state of charge must be included in the control of the motor converter.

A key element of the study was to set up a simulation project of the SOC estimation technique including coulomb counting with the use of the generic battery model.

From the results we can conclude that:

- ✓ The model of the battery used in MATLAB Simulink is less accurate in charging mode. However, it is very accurate and has good behavior of the battery during the discharging mode at a constant current. This is why often found in the literature for this mode. Indeed, this mode is very important that the charge mode especially in hybrid/electric vehicles applications.
- ✓ The estimator of the state of charge of the battery by Coulomb Counting method is very accurate and is widely used in practice especially in embedded applications type hybrid/electric vehicles or renewable energy applications in the case of photovoltaic systems for example.
- ✓ The disadvantage of this technique is its inaccuracy and the difficulty to find the initial SOC. Also, it requires high-precision measurement instruments (voltage, current, and temperature sensor); therefore, we have to calibrate these devices periodically.
- ✓ Lead acid batteries are really suitable only for vehicles of short range. They remain the cheapest type of battery per unit of stored energy, and they are likely to continue to be widely used for those purposes. Very many useful EVs that don't need a long range can be made.

So, by the simple calculation and simple hardware requirements, the proposed method can be easily implemented in all portable devices as well as electric vehicles.

In perspective, it would be interesting to:

- Work with batteries of other technologies (lithium)
- Test the techniques used in real time
- Use other estimation techniques (Artificial Neural Network, Kalman Filter, ...)
- Use two combined techniques (Coulomb couniting with OCV and Kalman Filter with OCV)

# APPENDICES

Appendix : The battery used in our project is of type **GPL 12520 12V 52Ah**


**Figure A.1:** *GPL 12520 12V 52Ah Battery Picture*

GPL 12520 is a general purpose battery up to 10 years in standby service or more than 260 cycles at 100% discharge in cycle service . As with all CSB batteries, all are rechargeable , highly efficient , leak proof and maintenance free.

## A.1.Specifications in Our Battery Model

| Specification | |
|---|---|
| Cells Per Unit | 6 |
| Voltage Per Unit | 12 |
| Capacity | 52 Ah @ 20hr-rate to 1.75V per cell @25°C (77°F) |
| Weight | Approx. 18 kg(39.68 lbs) |
| Maximum Discharge Current | 500A(5sec) |
| Internal Resistance | Approx. 5.5 mΩ |
| Operating Temperature Range | Discharge: -15°C~50°C ( 5°F~122°F)<br>Charge: -15°C~40°C ( 5°F~104°F)<br>Storage: -15°C~40°C ( 5°F~104°F) |
| Nominal Operating Temperature Range | 25°C±3°C ( 77°F±5°F) |
| Float Charging Voltage | 13.5 to 13.8 VDC/unit Average at 25°C (77°F) |
| Recommended Maximum Charging Current Limit | 15.6A |
| Equalization and Cycle Service | 14.4 to 15.0 VDC/unit Average at 25°C (77°F) |
| Self Discharge | CSB Batteries can be stored for more than 6 months at 25°C (77°F). Please charge batteries before using . For higher temperatures the time interval will be shorter. |
| Terminal | B4-L terminal to accept M6 nut & bolt |
| Container Material | Polypropylene(UL 94-V0/File E50955)*Flammability resistance of (UL 94-HB/File E216959) can be available upon request. |

**Figure A.2:** *Specifications in Our Battery Model*

## A.2. Charging and Discharging Procedure

**Table A.1:** *Charging Procedure.*

| Application | Charge Voltage(V/Cell) | | | Max.Charge Current |
|---|---|---|---|---|
| | Temperature | Set Point | Allowable Range | |
| Cycle Use | 25℃(77℉) | 2.45 | 2.40~2.50 | 0.3C |
| Standby | 25℃(77℉) | 2.275 | 2.25~2.30 | |

**Table A.2:** *Discharge Current VS Discharge Voltage.*

| Final Discharge Voltage V/Cell | 1.75 | 1.70 | 1.60 | 1.30 |
|---|---|---|---|---|
| Discharge Current(A) | 0.2C>(A) | 0.2C<(A)<0.5C | 0.5C<(A)<1.0C | (A)>1.0C |

## A.3. Battery Curves

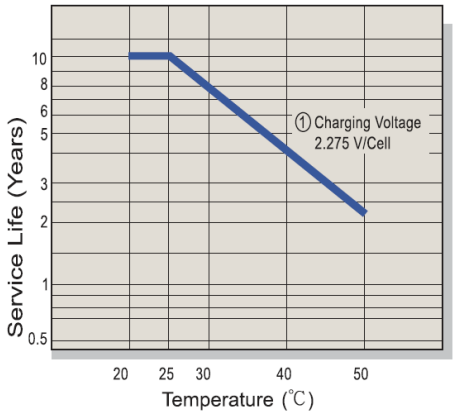


**Figure A.3:** *Float Service Life*

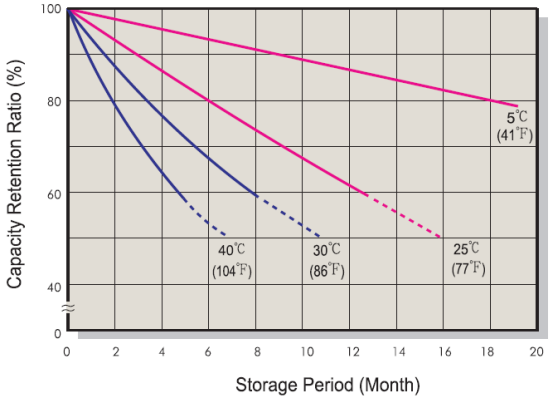


**Figure A.4:** *Capacity Retention Characteristic*

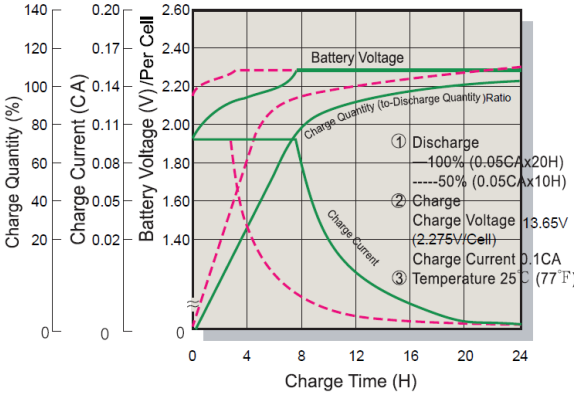


**Figure A.5:** *Battery Voltage and Charge Time for Standby Use*

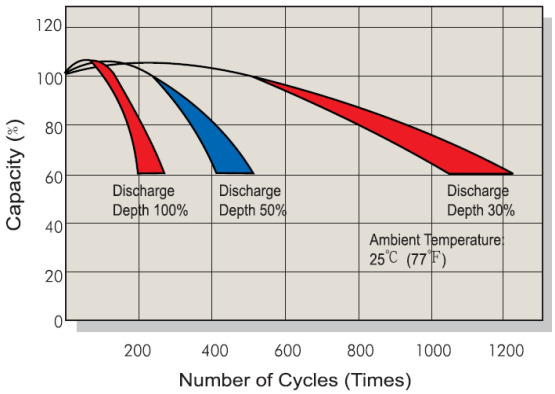


**Figure A.6:** *Cycle Service Life*

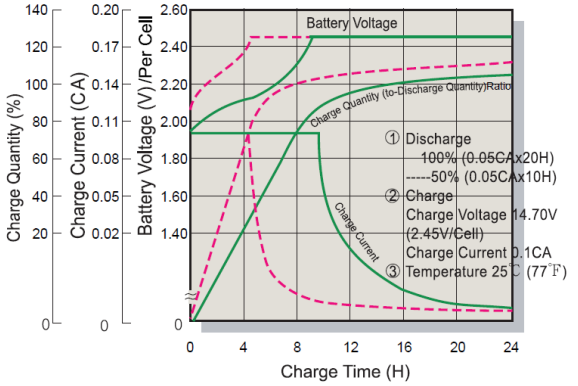


**Figure A.7:** *Battery Voltage and Charge Time for Cycle Use*

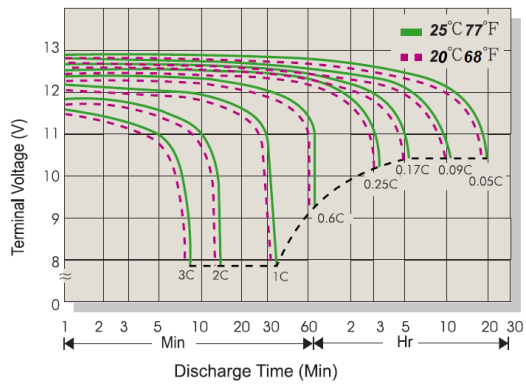


**Figure A.8:** *Terminal Voltage (V) and Discharge Time*

# References

# References


[1] D. Andrea, *Battery management systems for large lithium ion battery packs*. Artech house, 2010.

[2] Z.-Y. Hou, P.-Y. Lou, and C.-C. Wang, "State of charge, state of health, and state of function monitoring for EV BMS," in *2017 IEEE International Conference on Consumer Electronics (ICCE)*, 2017, pp. 310-311: IEEE.

[3] L. Lu, X. Han, J. Li, J. Hua, and M. Ouyang, "A review on the key issues for lithium-ion battery management in electric vehicles," *Journal of power sources,* vol. 226, pp. 272-288, 2013.

[4] H. J. Bergveld, W. S. Kruijt, and P. H. Notten, "Battery management systems," in *Battery Management Systems*: Springer, 2002, pp. 9-30.

[5] M. W. Verbrugge, E. D. Tate Jr, S. D. Sarbacker, and B. J. Koch, "Quasi-adaptive method for determining a battery's state of charge," ed: Google Patents, 2002.

[6] S. Rodrigues, N. Munichandraiah, and A. Shukla, "A review of state-of-charge indication of batteries by means of ac impedance measurements," *Journal of power Sources,* vol. 87, no. 1-2, pp. 12-20, 2000.

[7] B. A. Johnson and R. E. White, "Characterization of commercially available lithium-ion batteries," *Journal of power sources,* vol. 70, no. 1, pp. 48-54, 1998.

[8] J. H. Aylor, A. Thieme, and B. Johnso, "A battery state-of-charge indicator for electric wheelchairs," *IEEE transactions on industrial electronics,* vol. 39, no. 5, pp. 398-409, 1992.

[9] F. A. Schoofs, W. S. Kruijt, R. E. Einerhand, S. A. Hanneman, and H. J. Bergveld, "Method of and device for determining the charge condition of a battery," ed: Google Patents, 2002.

[10] V. Pop, H. J. Bergveld, D. Danilov, P. P. Regtien, and P. H. Notten, *Battery management systems: Accurate state-of-charge indication for battery-powered applications*. Springer Science & Business Media, 2008.

[11] F. Huet, "A review of impedance measurements for determination of the state-of-charge or state-of-health of secondary batteries," *Journal of power sources,* vol. 70, no. 1, pp. 59-69, 1998.

[12] J. Garche and A. Jossen, "Battery management systems (BMS) for increasing battery life time," in *TELESCON 2000. Third International Telecommunications Energy Special Conference (IEEE Cat. No. 00EX424)*, 2000, pp. 81-88: IEEE.

[13] G. L. Plett, "Extended Kalman filtering for battery management systems of LiPB-based HEV battery packs :Part 3. State and parameter estimation," *Journal of Power sources,* vol. 134, no. 2, pp. 277-292, 2004.

[14] G. L. Plett, "Extended Kalman filtering for battery management systems of LiPB-based HEV battery packs: Part 2. Modeling and identification," *Journal of power sources,* vol. 134, no. 2, pp. 262-276, 2004.

[15] O. Gérard, J.-N. Patillon, and F. d'Alché-Buc, "Neural network adaptive modeling of battery discharge behavior," in *International Conference on Artificial Neural Networks*, 1997, pp. 1095-1100 :Springer.

[16] S. Grewal and D. Grant, "A novel technique for modelling the state of charge of lithium ion batteries using artificial neural networks," 2001.

[17] A. J. Salkind, C. Fennie, P. Singh, T. Atwater, and D. E. Reisner, "Determination of state-of-charge and state-of-health of batteries by fuzzy logic methodology," *Journal of Power sources,* vol. 80, no. 1-2, pp. 293-300, 1999.

[18] S. Piller, M. Perrin, and A. Jossen, "Methods for state-of-charge determination and their applications," *Journal of power sources,* vol. 96, no. 1, pp. 113-120, 2001.

[19] S. Boschert, *Plug-in hybrids: The cars that will recharge America*. New Society Publishers, 2006.

[20] S. Boschert, *Plug-in hybrids: The cars that will recharge America*. New Society Publishers, 2006.

[21] S. Al-Hallaj and J. R. Selman, "Thermal modeling of secondary lithium batteries for electric vehicle/hybrid electric vehicle applications," *Journal of power sources,* vol. 110, no. 2, pp. 341-348, 2002.

[22] D. H. Doughty, P. C. Butler, A. A. Akhil, N. H. Clark, and J. D. Boyes, "Batteries for large-scale stationary electrical energy storage," *The Electrochemical Society Interface,* vol. 19, no. 3, pp. 49-53, 2010.

[23] Y. Onoda, "Development of a large-sized, long-life, valve-regulated lead–acid battery," *Journal of power sources,* vol. 88, no. 1, pp. 101-107, 2000.

[24] J. Jiang and C. Zhang, *Fundamentals and applications of lithium-ion batteries in electric drive vehicles*. John Wiley & Sons, 2015.

[25] C. Glaize and S. Genies, *Lithium batteries and other electrochemical storage systems*. Wiley Online Library, 2013.

[26] R. Korthauer, "Areas of activity on the fringe of lithium-ion battery development, production, and recycling," in *Lithium-Ion Batteries: Basics and Applications*: Springer, 2018, pp. 249-251.

[27] M. E. Spahr *et al.*, "Purely hexagonal graphite and the influence of surface modifications on its electrochemical lithium insertion properties," *Journal of The Electrochemical Society,* vol. 149, no. 8, pp. A960-A966, 2002.

[28] J. Garche, C. K. Dyer, P. T. Moseley, Z. Ogumi, D. A. Rand, and B. Scrosati, *Encyclopedia of electrochemical power sources*. Newnes, 2013.

[29] D. Pavlov, *Lead-acid batteries: science and technology*. Elsevier, 2011.

[30] D. Linden, "Reddy TB handbook of batteries," ed: The McGraw-Hill Companies, Inc., New York, 2002.

[31] T. Ikeya *et al.*, "Multi-step constant-current charging method for an electric vehicle nickel/metal hydride battery with high-energy efficiency and long cycle life," *Journal of power sources,* vol. 105, no. 1, pp. 6-12, 2002.

[32] C.-L. Liu, S.-C. Wang, Y.-H. Liu, and M.-C. Tsai, "An optimum fast charging pattern search for Li-ion batteries using particle swarm optimization," in *The 6th International Conference on Soft Computing and Intelligent Systems, and The 13th International Symposium on Advanced Intelligence Systems*, 2012, pp. 727-732: IEEE.

[33] Y.-H. Liu, C.-H. Hsieh, and Y.-F. Luo, "Search for an optimal five-step charging pattern for Li-ion batteries using consecutive orthogonal arrays," *IEEE Transactions on Energy Conversion*, vol. 26, no. 2, pp. 654-661, 2011.

[34] P. H. Notten, J. O. het Veld, and J. Van Beek, "Boostcharging Li-ion batteries: A challenging new charging concept," *Journal of Power Sources*, vol. 145, no. 1, pp. 89-94, 2005.

[35] C.-H. Lin *et al.*, "Fast charging technique for Li-Ion battery charger," in *2008 15th IEEE International Conference on Electronics, Circuits and Systems*, 2008, pp. 618-621: IEEE.

[36] L.-R. Chen, "Design of duty-varied voltage pulse charger for improving Li-ion battery-charging response," *IEEE Transactions on Industrial Electronics*, vol. 56, no. 2, pp. 480-487, 2008.

[37] T. T. Vo, X. Chen, W. Shen, and A. Kapoor, "New charging strategy for lithium-ion batteries based on the integration of Taguchi method and state of charge estimation," *Journal of Power Sources*, vol. 273, pp. 413-422, 2015.

[38] L.-R. Chen, S.-L. Wu, T.-R. Chen, W.-R. Yang, C.-S. Wang, and P.-C. Chen, "Detecting of optimal Li-ion battery charging frequency by using AC impedance technique," in *2009 4th IEEE Conference on Industrial Electronics and Applications*, 2009, pp. 3378-3381: IEEE.

[39] L.-R. Chen, S.-L. Wu, D.-T. Shieh, and T.-R. Chen, "Sinusoidal-ripple-current charging strategy and optimal charging frequency study for Li-ion batteries," *IEEE Transactions on Industrial Electronics*, vol. 60, no. 1, pp. 88-97, 2012.

[40] Q. Gong, "Modeling study of a vehicle traction battery model," *Chinese LABAT Man*, vol. 42, no. 2, p. 76, 2005.

[41] M. Ceraolo, "New dynamical models of lead-acid batteries," *IEEE transactions on Power Systems*, vol. 15, no. 4, pp. 1184-1190, 2000.

[42] F. M. González-Longatt, "Circuit based battery models: A review," in *Congreso Iberoamericano de estudiantes De Ingenieria Electrica. Cibelec*, 2006.

[43] H. Fakham, D. Lu, and B. Francois, "Power control design of a battery charger in a hybrid active PV generator for load-following applications," *IEEE Transactions on Industrial Electronics*, vol. 58, no. 1, pp. 85-94, 2010.

[44] V. Johnson, "Battery performance models in ADVISOR," *Journal of power sources*, vol. 110, no. 2, pp. 321-329, 2002.

[45] B. A. Manual, "Gates Energy Products," *Inc., Gainesville, FL*, 1989.

[46] J. P. Christophersen *et al.*, "DOE Advanced technology development program for lithium-ion batteries: INEEL Interim report for Gen 2 cycle-life testing," *9: INEEL/EXT-02-01055*, 2002.

[47] S. Wu, R. Xiong, H. Li, V. Nian, and S. Ma, "The state of the art on preheating lithium-ion batteries in cold weather," *Journal of Energy Storage*, vol. 27, p. 101059, 2020.

[48] J. Huang, Z. Li, B. Y. Liaw, and J. Zhang, "Graphical analysis of electrochemical impedance spectroscopy data in Bode and Nyquist representations," *Journal of Power Sources,* vol. 309, pp. 82-98, 2016.

[49] B. Wang, Z. Liu, S. E. Li, S. J. Moura, and H. Peng, "State-of-charge estimation for lithium-ion batteries based on a nonlinear fractional model," *IEEE Transactions on Control Systems Technology,* vol. 25, no. 1, pp. 3-11, 2016.

[50] R. Yang, R. Xiong, H. He, and Z. Chen, "A fractional-order model-based battery external short circuit fault diagnosis approach for all-climate electric vehicles application," *Journal of cleaner production,* vol. 187, pp. 950-959, 2018.

[51] I. Petráš, *Fractional-order nonlinear systems: modeling, analysis and simulation*. Springer Science & Business Media, 2011.

[52] G. R. Dahlin and K. E. Strøm, *Lithium batteries: research, technology, and applications*. Nova Science Publishers, 2010.

[53] M. Faizan, "Synthesis and Characterization of Lead based Anodic Electrode for Lead Acid Batteries," Department of Physics, COMSATS University Islamabad, Lahore campus, 2019.

[54] D. Doerffel and S. A. Sharkh, "A critical review of using the Peukert equation for determining the remaining capacity of lead-acid and lithium-ion batteries," *Journal of power sources,* vol. 155, no. 2, pp. 395-400, 2006.

[55] G. Albright, J. Edie, and S. Al-Hallaj, "A comparison of lead acid to lithium-ion in stationary storage applications," *Published by AllCell Technologies LLC,* 2012.

[56] H. Chang and H. Wu, "Graphene-based nanocomposites: preparation, functionalization, and energy and environmental applications," *Energy & Environmental Science,* vol. 6, no. 12, pp. 3483-3507, 2013.

[57] H. Keshan, J. Thornburg, and T. S. Ustun, "Comparison of lead-acid and lithium ion batteries for stationary storage in off-grid energy systems," 2016.

[58] E. M. Krieger, J. Cannarella, and C. B. Arnold, "A comparison of lead-acid and lithium-based battery behavior and capacity fade in off-grid renewable charging applications," *Energy,* vol. 60, pp. 492-500, 2013.

[59] O. S. W. Al-Qasem, "Modeling and simulation of lead-acid storage batteries within photovoltaic power systems," *A Thesis Presented to the An-Najah National University, Palestine,* 2012.

[60] P. Ng, T. Nguyen, M. Weeks, A. Cannone, and K. Bullock, "Performance and characteristics of valve regulated lead acid batteries with a concentric square grid design," in *Proceedings of Intelec 93: 15th International Telecommunications Energy Conference,* 1993, vol. 2, pp. 115-122: IEEE.

[61] A. Devie, "Caractérisation de l'usage des batteries Lithium-ion dans les véhicules électriques et hybrides. Application à l'étude du vieillissement et de la fiabilité," 2012.

[62] B. Scrosati, K. Abraham, W. A. van Schalkwijk, and J. Hassoun, *Lithium batteries: advanced technologies and applications*. John Wiley & Sons, 2013.

[63] A. Kirchev, A. Delaille, M. Perrin, E. Lemaire, and F. Mattera, "Studies of the pulse charge of lead-acid batteries for PV applications: Part II. Impedance of the positive plate revisited," *Journal of Power Sources,* vol. 170, no. 2, pp. 495-512, 2007.

[64] B. Zine, K. Marouani, M. Becherif, and S. Yahmedi, "Estimation of battery SOC for hybrid electric vehicle using coulomb counting method," *International Journal of Emerging Electric Power Systems,* vol. 19, no. 2, 2018.

[65] D. DinhVinh, "Lithium-Ion batteries diagnosis in embedded applications," *ThesisforobtainingthedegreeofdoctorofCompiegneUniversityof TechnologyinInformationTechnologyandSystems,* 2010.

[66] X. Hu, F. Sun, and Y. Zou, "Estimation of state of charge of a lithium-ion battery pack for electric vehicles using an adaptive Luenberger observer," *Energies,* vol. 3, no. 9, pp. 1586-1603, 2010.

[67] D. Lindner and F. Niedermayr, "Report for work package 6," ed: FRAUNHOFR-ITALIA, 2014.

[68] K. S. Ng, C.-S. Moo, Y.-P. Chen, and Y.-C. Hsieh, "Enhanced coulomb counting method for estimating state-of-charge and state-of-health of lithium-ion batteries," *Applied energy,* vol. 86, no. 9, pp. 1506-1511, 2009.

[69] F. Feng, R. Lu, and C. Zhu, "A combined state of charge estimation method for lithium-ion batteries used in a wide ambient temperature range," *Energies,* vol. 7, no. 5, pp. 3004-3032, 2014.

[70] O. Tremblay and L.-A. Dessaint, "Experimental validation of a battery dynamic model for EV applications," *World electric vehicle journal,* vol. 3, no. 2, pp. 289-298, 2009.

[71] S. Wijewardana, "New Dynamic Battery Model for Hybrid Vehicles and Dynamic Model Analysis Using Simulink," *Engineer: Journal of the Institution of Engineers, Sri Lanka,* vol. 47, no. 4, 2014.

[72] E. M. Allam, "Study vehicle battery simulation and monitoring system," *American Journal of Modeling and Optimization,* vol. 3, no. 2, pp. 40-49, 2015.

[73] S. Xu, Z. Yan, X. Zhao, L. Zhang, D. Feng, and X. Xu, "Decentralized charging of plug-in electric vehicles using lagrange relaxation method at the residential transformer level," *International Journal of Emerging Electric Power Systems,* vol. 17, no. 3, pp. 267-276, 2016.

[74] B. Zine, K. Marouani, M. Becherif, and S. Yahmedi, "Estimation of battery SOC for hybrid electric vehicle using coulomb counting method," *International Journal of Emerging Electric Power Systems,* vol. 19, no. 2, 2018.

[75] S. Xu, Z. Yan, X. Zhao, L. Zhang, D. Feng, and X. Xu, "Decentralized charging of plug-in electric vehicles using lagrange relaxation method at the residential transformer level," *International Journal of Emerging Electric Power Systems,* vol. 17, no. 3, pp. 267-276, 2016.

[76] R. Baroody, "Evaluation of rapid electric battery charging techniques," 2009.

**Titre du mémoire :** ETUDE DES TECHNIQUES D'ESTIMATION DE L'ETAT DE CHARGE DE LA BATTERIE D'UN SYSTEME EMBARQUE.
**Master :** Electromécanique

**Auteur :** BIA Haithem, KHADEM Bachir et BELLILI Sifeddine.

**Mots clés :** Véhicule Electrique, Etat de Charge (SOC), Modèle générique de Batterie, Méthode de Comptage Coulométrique.

**Résumé :**

Les batteries au plomb ont acquis une énorme popularité en tant qu'éléments de stockage d'énergie pour la grande majorité des systèmes électriques rechargeables, y compris les véhicules électriques. Pour rendre les batteries au plomb plus sûres et plus fiables, un grand nombre de modèles de batteries ont été développés pour estimer leur état de charge actuel (SOC) où le SOC détermine la distance parcourue des véhicules électriques.
L'objectif principal de cette thèse est l'analyse des modèles de batteries populaires trouvés et de ses différents modèles dans le but de créer un modèle facile et efficace pour travailler l'approche avec la voiture électrique, et de fournir une base pour le développement de stratégies intelligentes de contrôle et d'estimation qui signifie développer un estimateur de charge de batterie basé sur une série de charge / décharge. Ainsi, nous avons utilisé dans cette étude la technique d'estimation du comptage coulométrique pour augmenter la précision de l'estimation.

---

**Thesis title:** ESTIMATING STATE OF CHARGE TECHNIQUES STUDY IN THE BATTERY OF AN EMBADDED SYSTEM.

**Keywords:** Electric Vehicle, State of Charge (SOC), Battery Generic Model, Coulomb Counting Method.

**Abstract:**

Lead acid batteries have gained enormous popularity as energy storage elements for the vast majority of rechargeable electric systems, including electric vehicles. To make Lead acid batteries safer and more reliable, a large number of battery models have been developed to estimate their current state of charge (SOC). Where the SOC determines the driving distance of electric vehicles.
The primary objective of this thesis is the analysis of popular battery models found and its various models with the aim of creating an easy and successful model for working the approach with the electric car, and to provide a foundation for developing intelligent control and estimation strategies that does mean develop a battery charge estimator based on series of charge/discharge . Thus, we used in this study estimation technique coulomb counting to increase estimation accuracy.

---

**عنوان المذكرة:** دراسة تقنيات تقدير حالة شحن بطارية على الأنظمة المضمنة

**الكلمات المفتاحية:** سيارة كهربائية، حالة الشحن، نموذج البطارية، طريقة عد كولومي

**الملخص:**1

اكتسبت بطاريات الرصاص الحمضية شعبية كبيرة كعناصر تخزين الطاقة للغالبية العظمى من الأنظمة الكهربائية القابلة لإعادة الشحن، بما في ذلك السيارات الكهربائية. لجعل بطاريات الرصاص الحمضية أكثر أمانًا وموثوقية، تم تطوير عدد كبير من نماذج البطاريات لتقدير حالة الشحن الحالية(SOC) ، حيث تحدد SOC مسافة القيادة للمركبات الكهربائية.

الهدف الأساسي من هذه الأطروحة هو تحليل نماذج البطاريات الشائعة الموجودة ونماذجها المختلفة بهدف إنشاء نموذج سهل وناجح للعمل مع النهج مع السيارة الكهربائية، وتوفير أساس لتطوير استراتيجيات التحكم والتقدير الذكية التي يعني تطوير مقدر لشحن البطارية بناءً على سلسلة الشحن / التفريغ. وهكذا، استخدمنا في هذه الدراسة تقنية تقدير عد كولومي لزيادة دقة التقدير.